QCD studies at LHC using CMS detector

Suvadeep Bose

Dept of High Energy Physics

Tata Institute of Fundamental Research

Work done under the supervision of

Prof. Sunanda Banerjee

Thesis Defense
September 28 , 2010

Outline

- Introduction
- CMS Detector
- Test Beam experiment
  - Particle Identification
  - Energy reconstruction – response and resolution of calorimeter
- QCD studies in CMS
  - Jets and Event Selection
- Multijet Studies
  - Topological variables under study
  - Detector effects
  - Systematic and sensitivity study
  - Comparison among different event generators
- Event Shapes
  - Definitions of variables
  - Study with jets from charged tracks
- Summary

Compact Muon Solenoid (CMS)

- Designed for proton-proton collision at 14 TeV.
- Physics goals at the LHC:
  - Search for Higgs, new physics signal at TeV scale.

Large Hadron Collider (LHC)

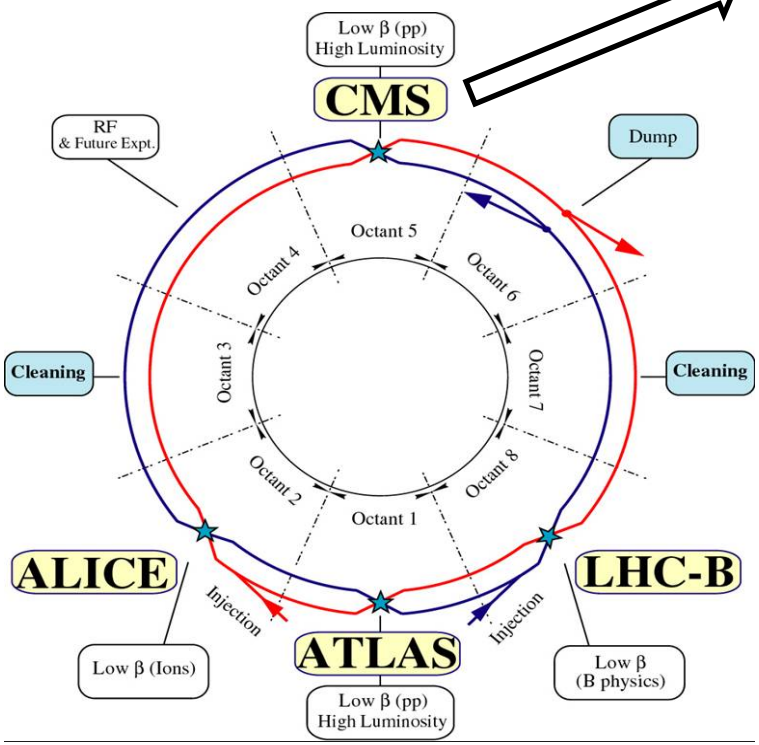

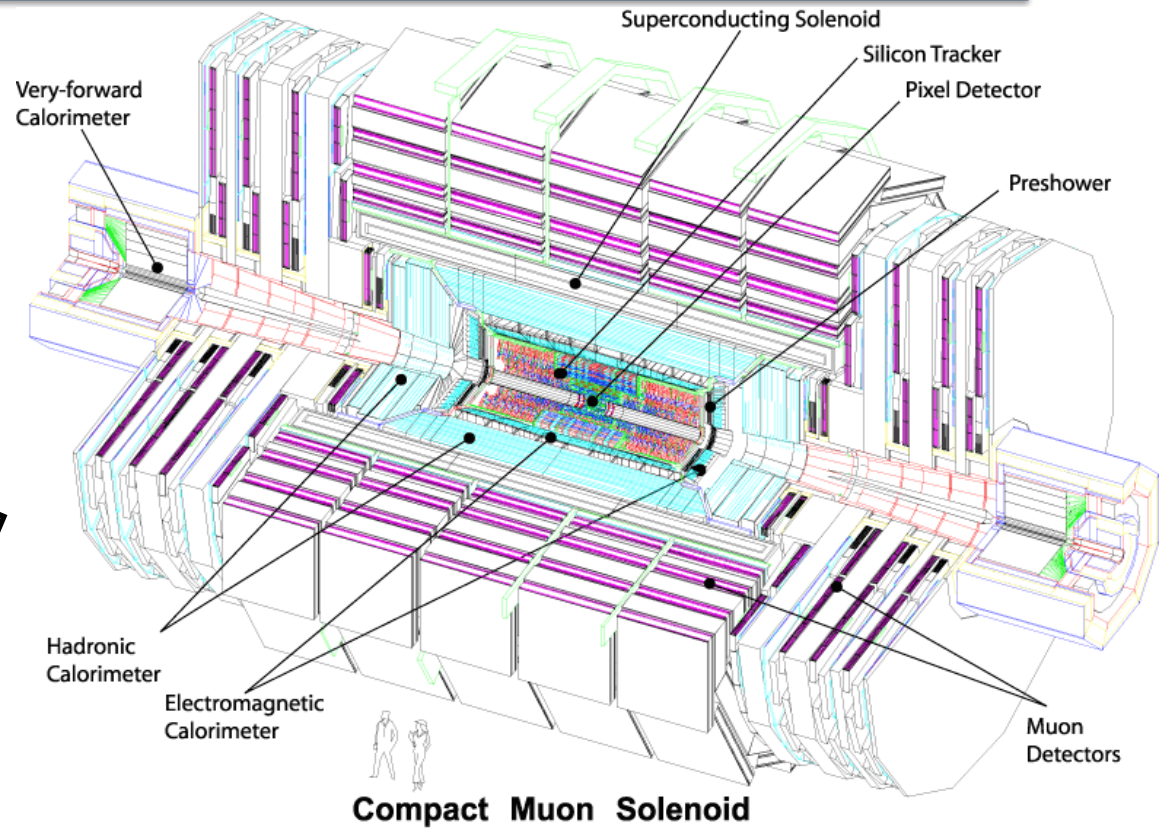

Polar angle **θ**
Azimuthal angle **φ**
Pseudorapidity **η** = -ln(tan θ/2)

- <u>CMS Detector components</u>:
  - Tracker
  - Calorimeter – ECAL + HCAL
  - Solenoid Magnet
  - Muon Chambers

Analysis of TestBeam 2007 data

Test Beam Experiment

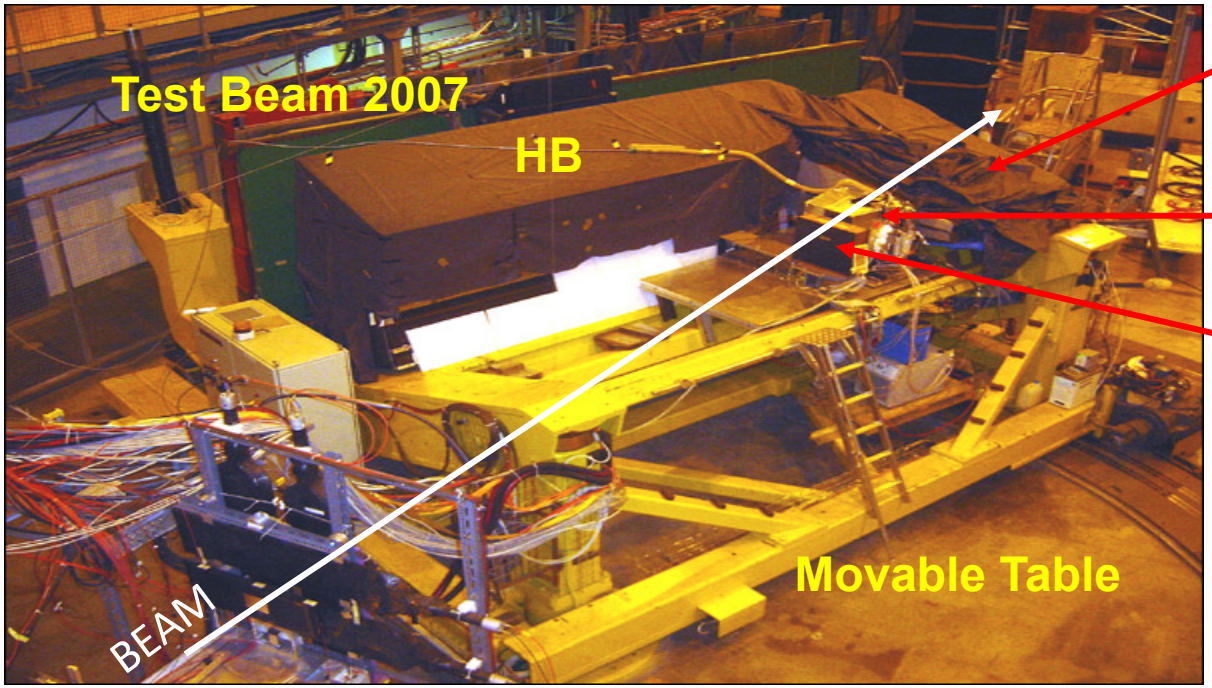

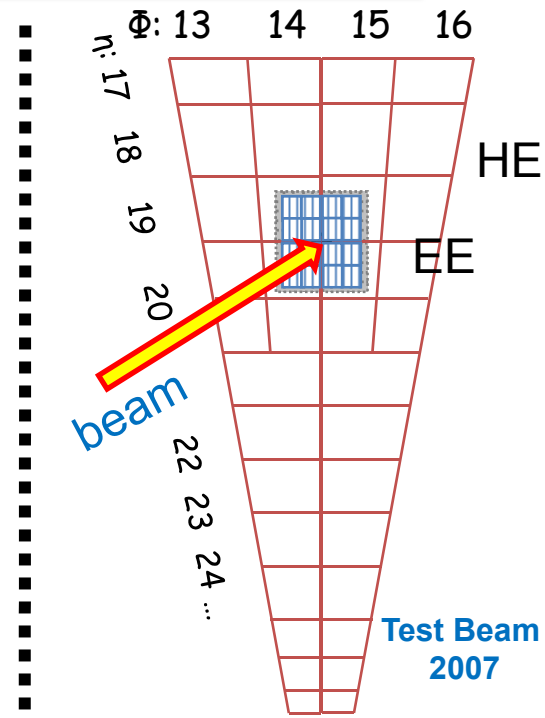

- Slice of CMS Calorimeter exposed to test beams at CERN H2 experimental area.
- Response and resolution of the calorimeter measured over a wide range of momenta of the hadrons (pions) [2-300 GeV/c].
- TB 2007 set up consisted of :
  - A prototype of one wedge of Hadron Endcap (HE)
  - Four super crystals of Electromagnetic Endcap (EE)
  - Preshower (ES).
- The complete set-up is mounted on a *movable table* such that the pivot of the table mimics the actual interaction point.

Beam Line Elements and particle identification

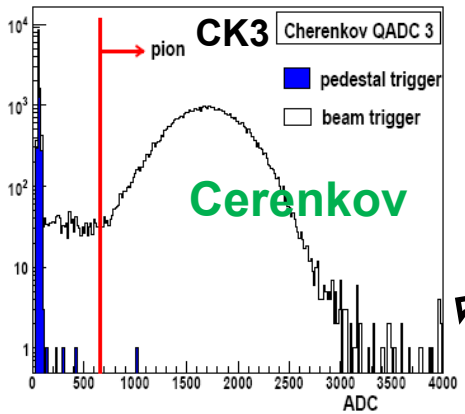

- Cerenkov counters (CK2, CK3) and Time of Flight (TOF) counters are used for particle identification.

Identifying π, p, k

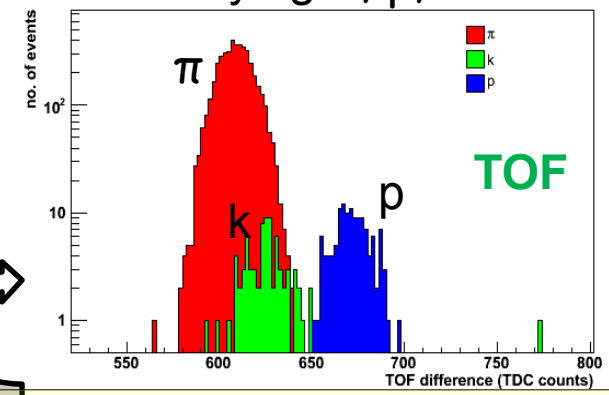

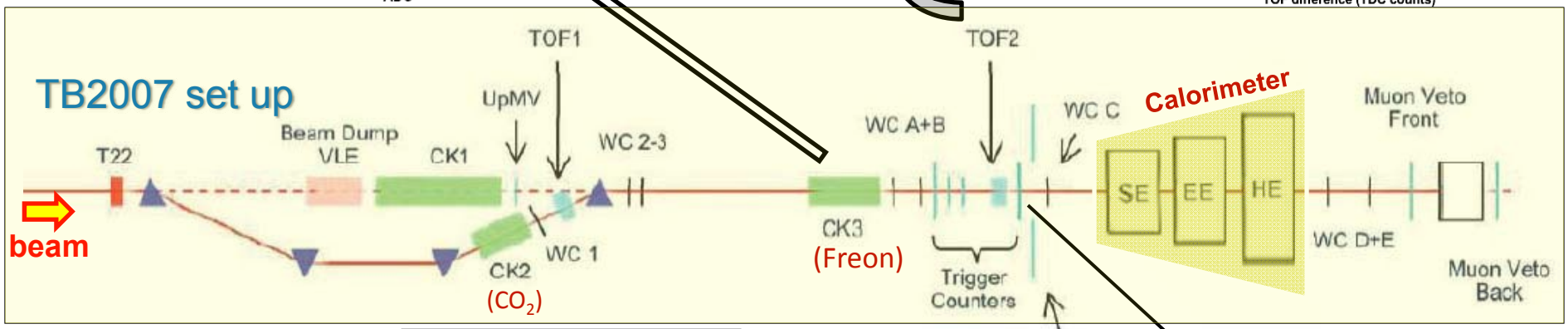

- Reject wide angle secondary produced in interactions with beam line elements using beam halo.

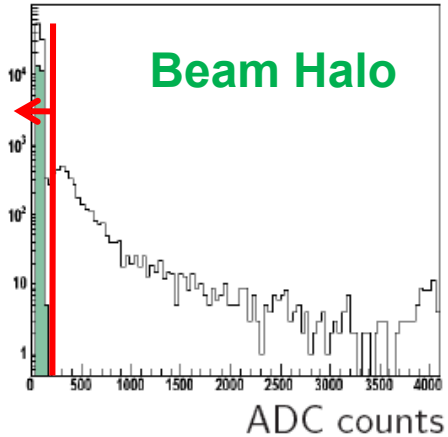

- Reject events with more than one particle in the trigger scintillator.

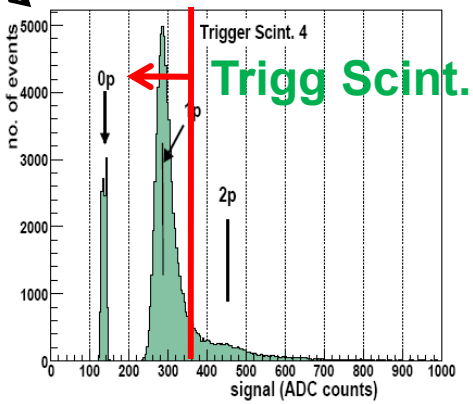

Study of Beam Profile of and material gap in EE

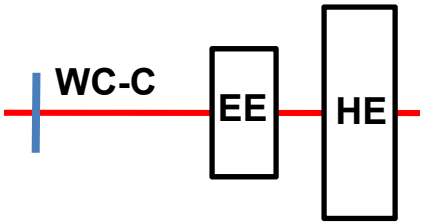

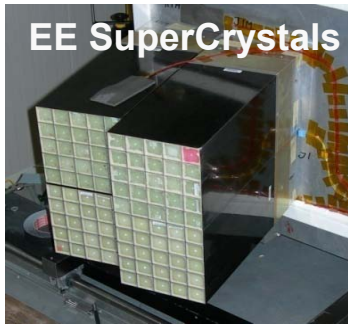

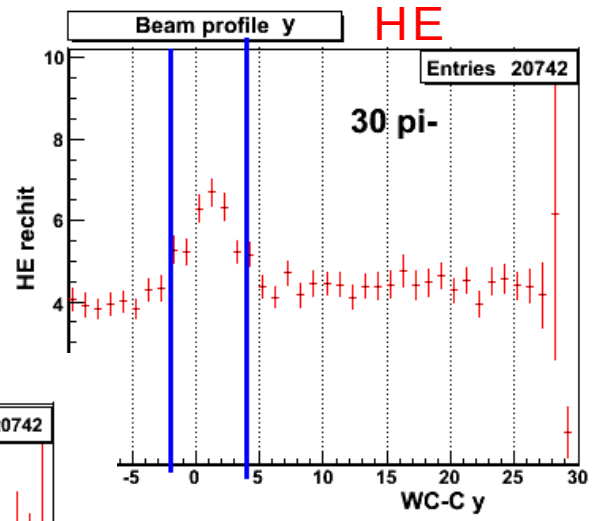

- A **dip** in the energy deposit in EE as a function of Wire chamber y position.

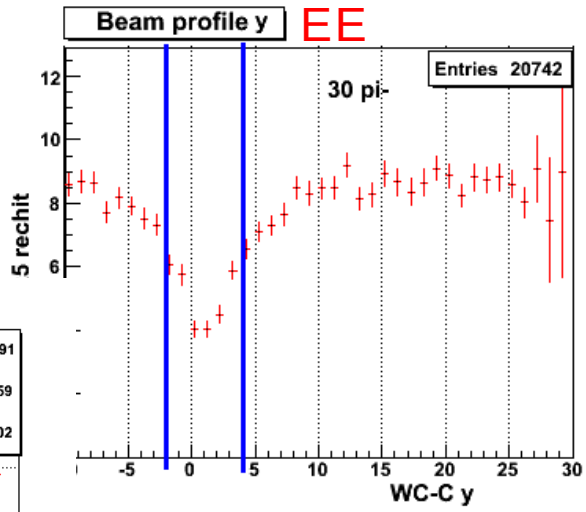

- A **peak** in the energy deposit in HE as a function of Wire chamber y position.

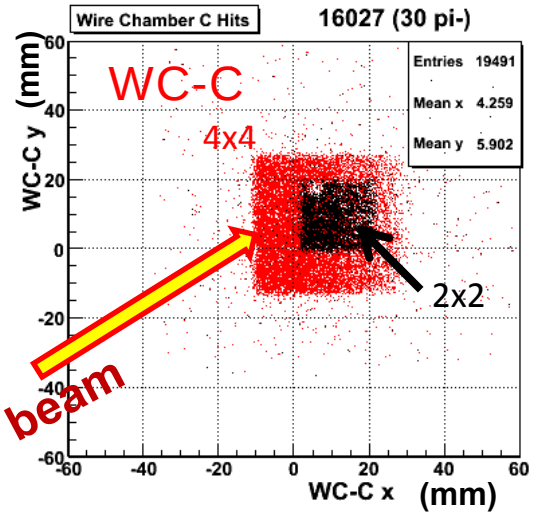

Wire chamber hits.

❑ **There was a gap in the boundary of two EE super crystals along y. Decision: to cut out events from y = - 2 mm to y = 4 mm in the Wire Chamber axis.**

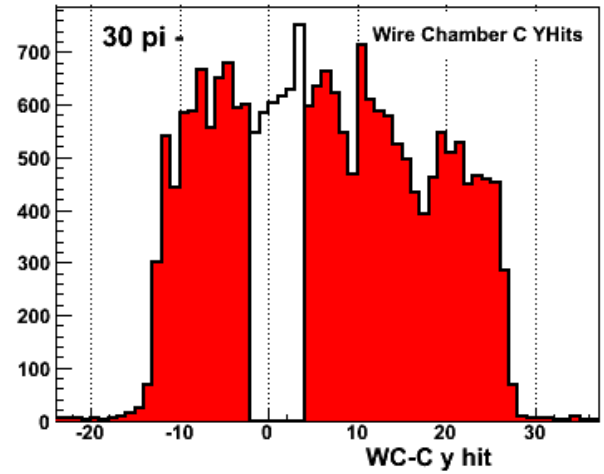

HCAL stand-alone case

Two depths in HE

Front (depth1)

Back (depth2)

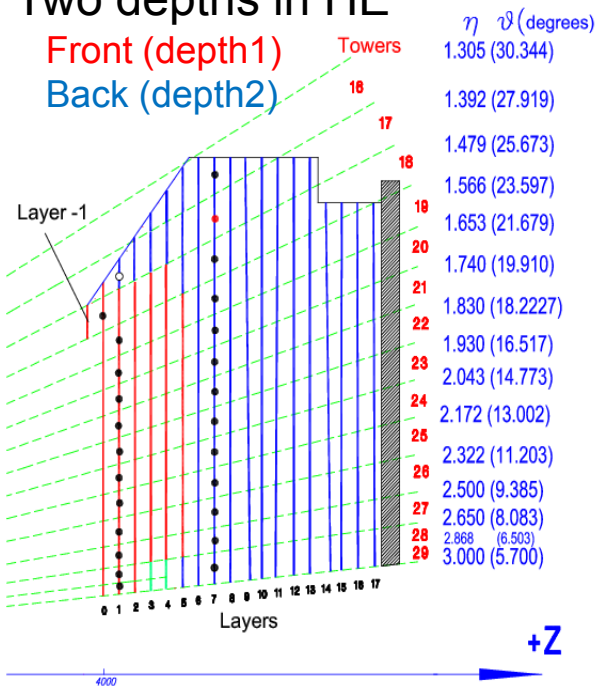

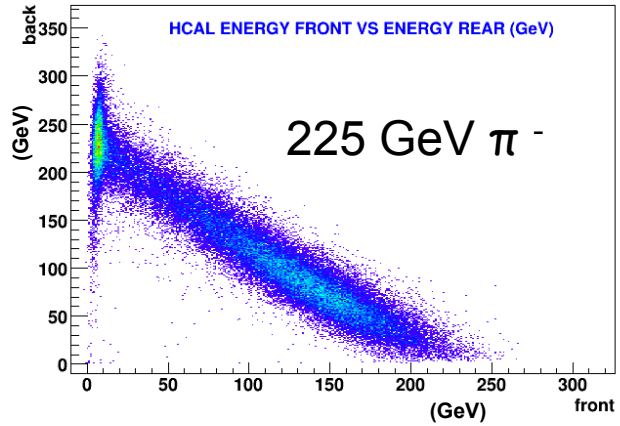

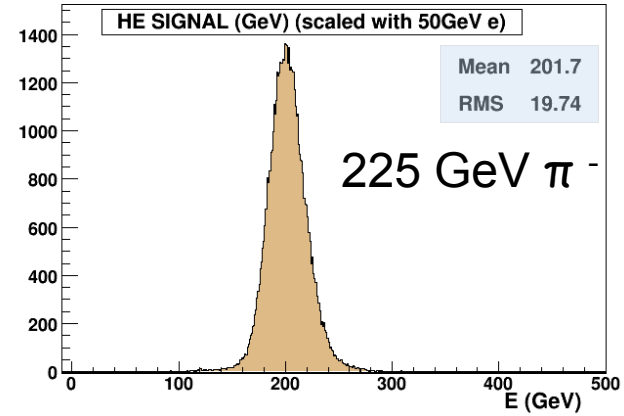

Energy sharing in Depth 1 and Depth 2 for HE
Straight line as same calorimeter.

Energy deposition for sum of two depths in HE.
4X4 towers around the beam spot are summed here.

- **Response and Resolution of HE stand alone.**
- **For p = 30-300 GeV/c response is ~0.9.**
- **Resolution for for HE alone:**

$$\frac{\sigma}{E} = \frac{92.0\%}{\sqrt{E}} \oplus 3.4\%$$

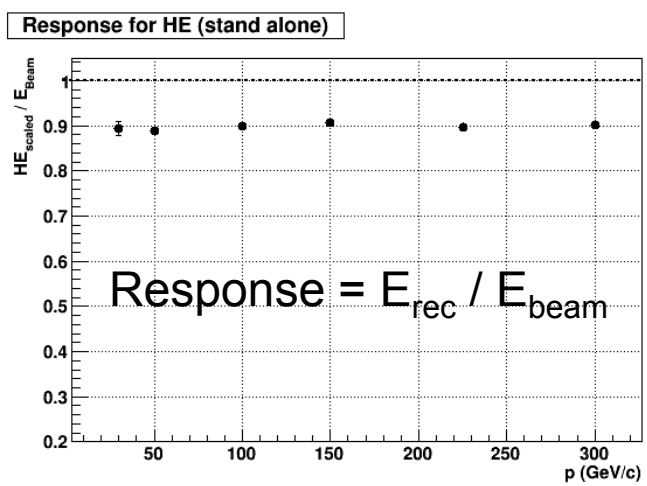

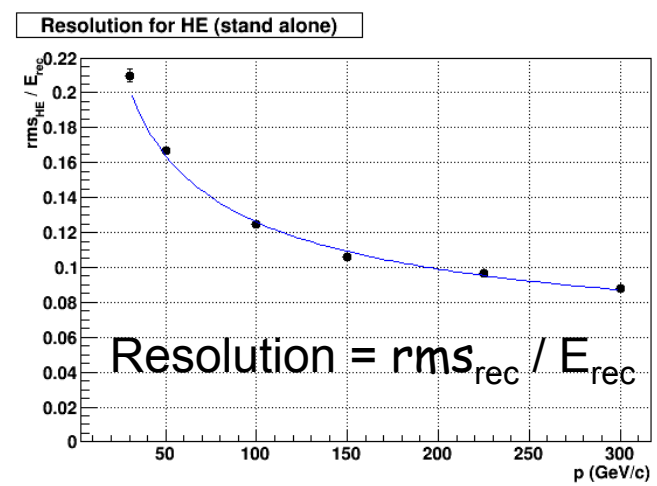

Energy measured in ECAL and HCAL

- Energy in ECAL is measured from 5x5 crystals and in HCAL from 4x4 towers.

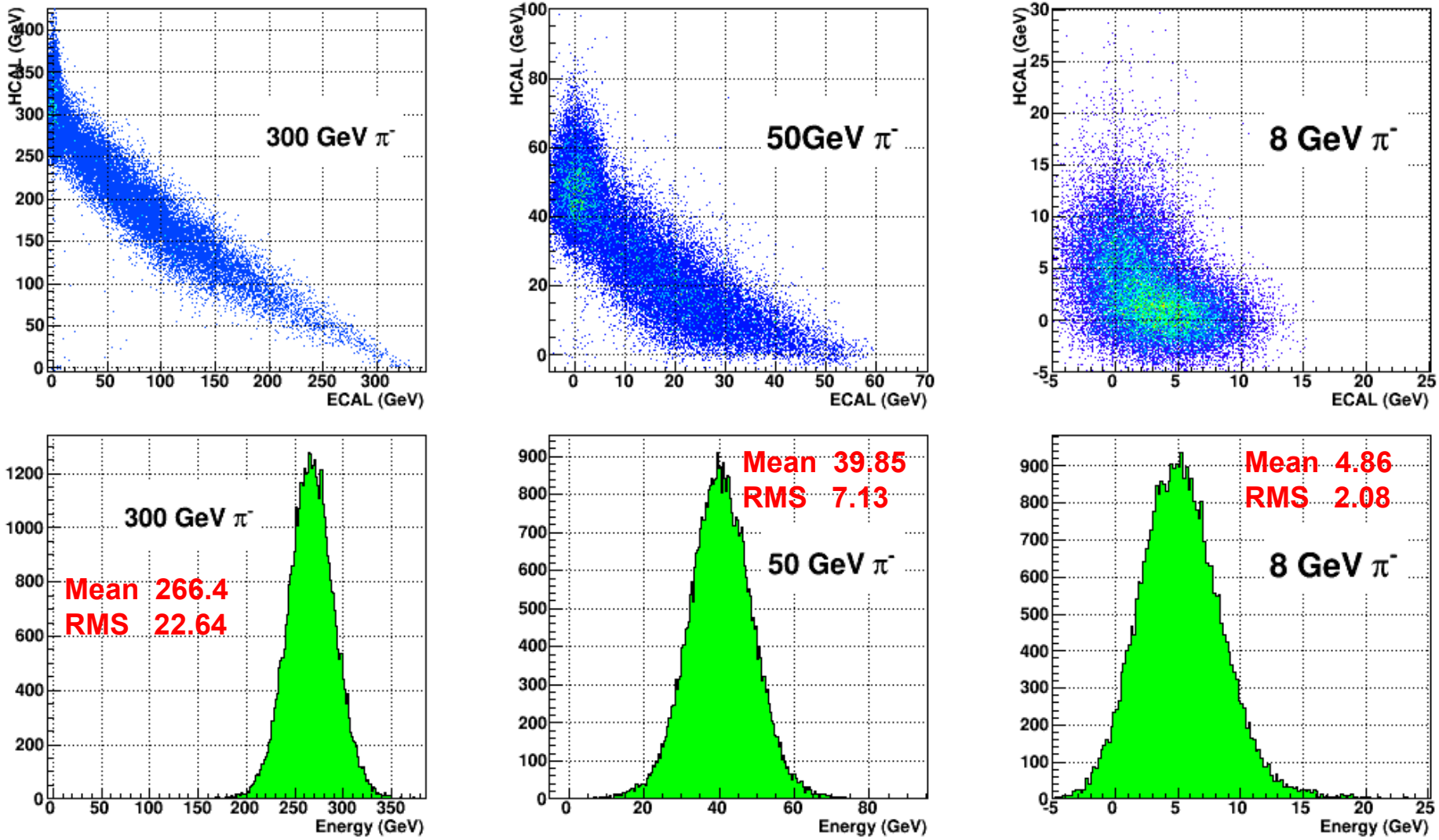

- Total energy : EE + HE (calibrated with 50 GeV e^-).

Response & Resolution of the Calorimeter - I

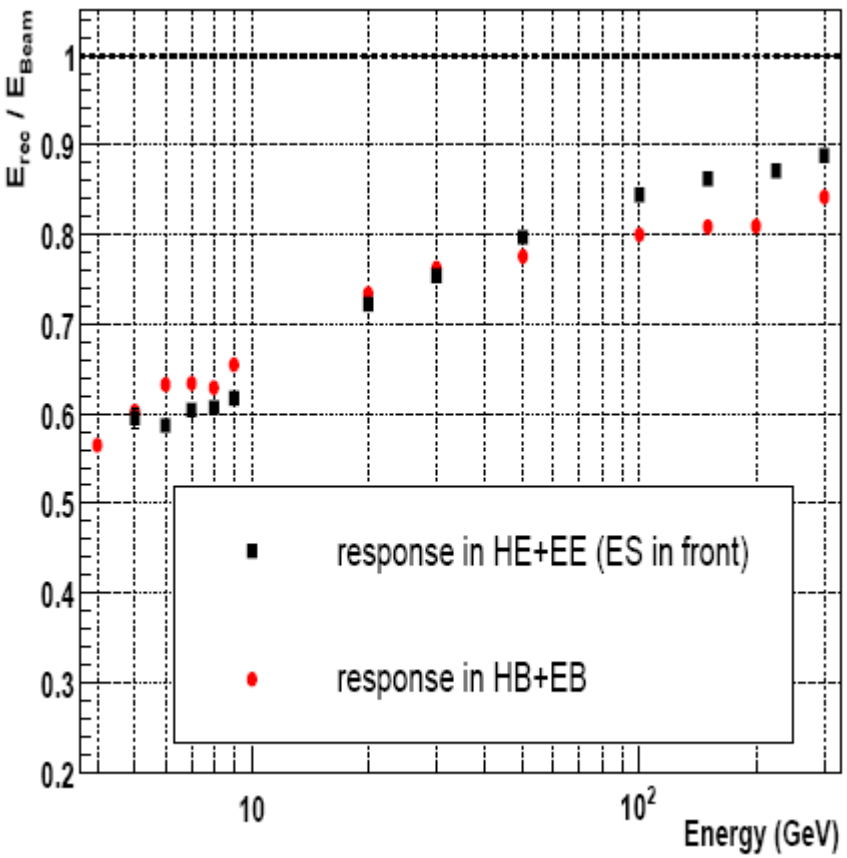

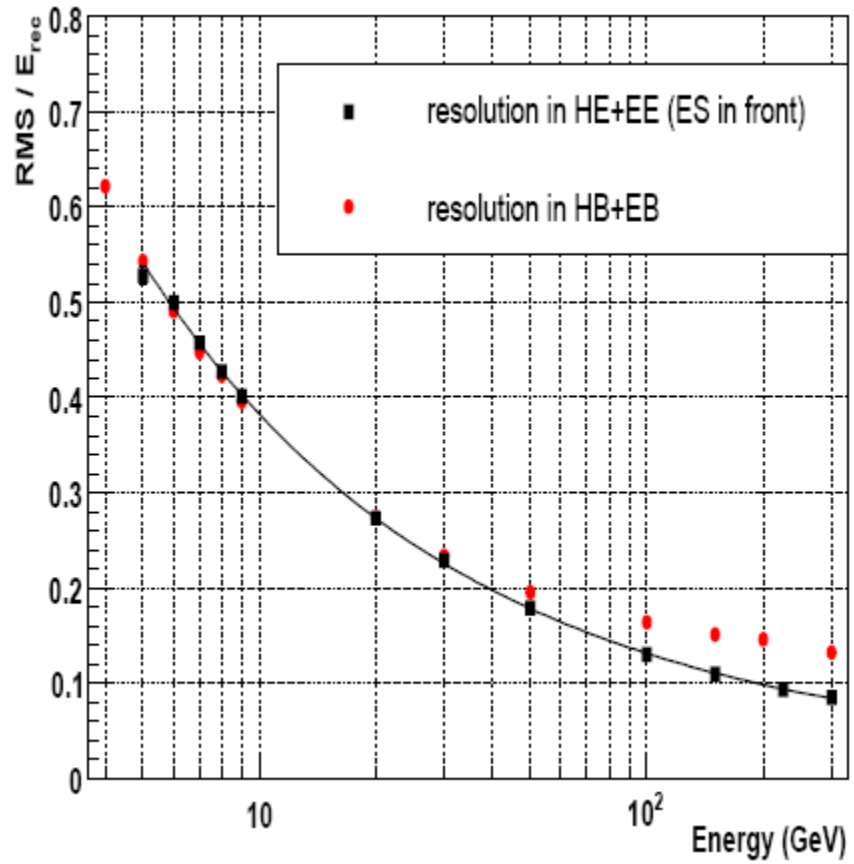

- We clearly see the non-linearity in the combined response which is similar for barrel and endcap.
- Resolution is also similar in barrel and in endcap in lower energies.
- Resolution is around 10% for 300 GeV and 20% for 30 GeV.

$$\frac{\sigma}{E} = \frac{a}{\sqrt{E}} \oplus b$$

For endcap:
a = 116.9% b = 1.4%

Response & Resolution of the Calorimeter - II

- **Consider particles for which energy measured in ECAL < 1.5 GeV to study HCAL alone system.**

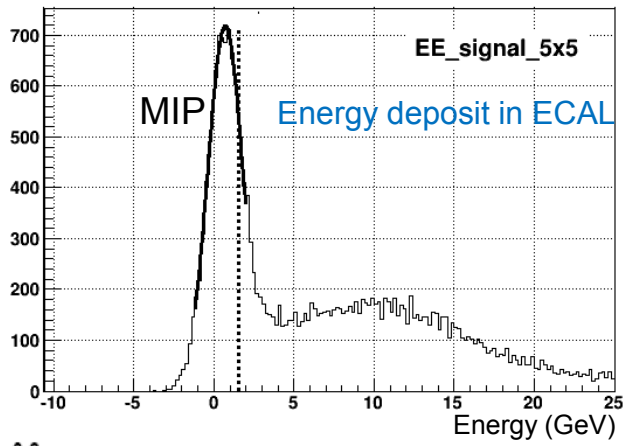

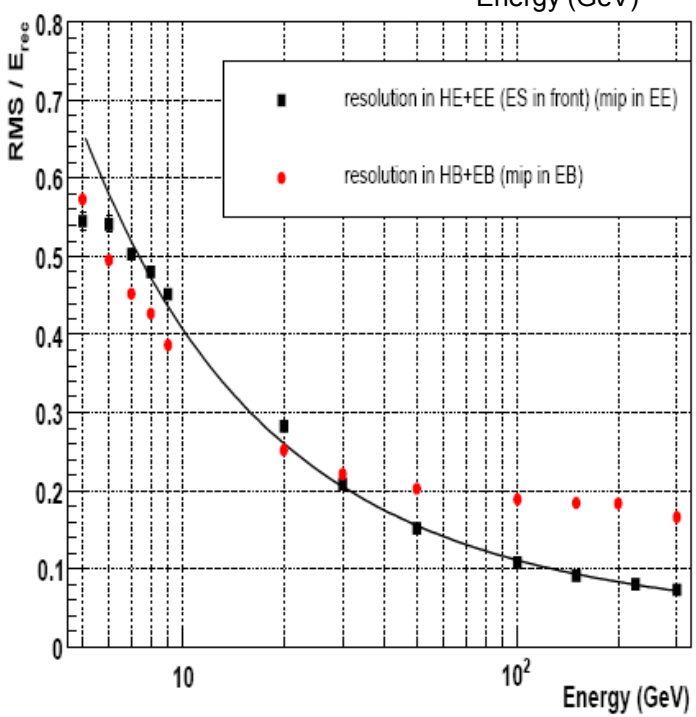

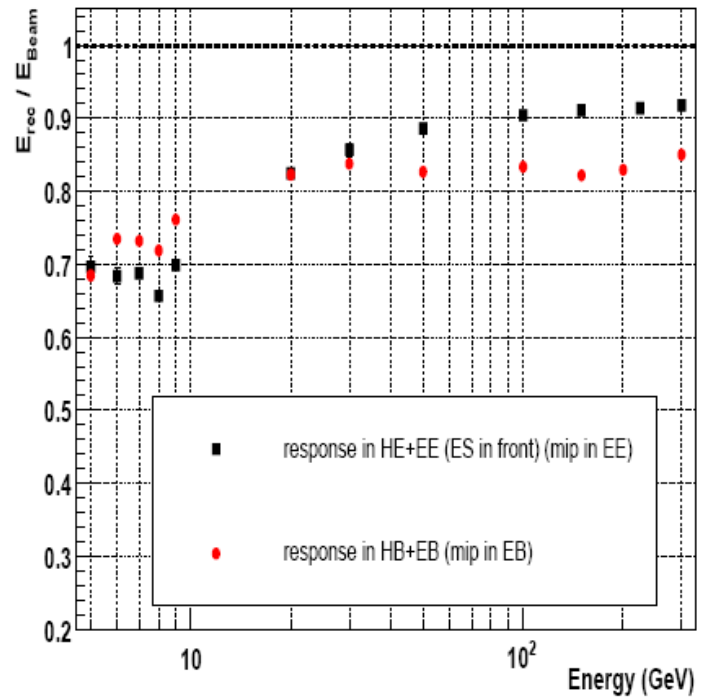

- ❑ The combined response is similar for barrel and endcap for low energies but response is higher in endcap for high energies.
- ❑ Resolution is better in endcap for higher energies.
- ❑ Resolution is worse in endcap for lower energies as determining MIP in EE is more difficult due to high noise.

QCD studies at LHC using CMS detector

- *All the plots are based on Monte Carlo samples as the LHC data were not available till the time of the analysis. The official Monte Carlo production was done at $\sqrt{s}$ =10 TeV as per plan for LHC till then.*

What are Jets?

- The Jets are the signature of partons, materialized as sprays of highly collimated hadrons.

- A calorimeter jet (**Calojets**) is the output of the jet finding algorithm when applied to the CaloTowers.

$$R = \sqrt{(\Delta\eta)^2 + (\Delta\varphi)^2}$$

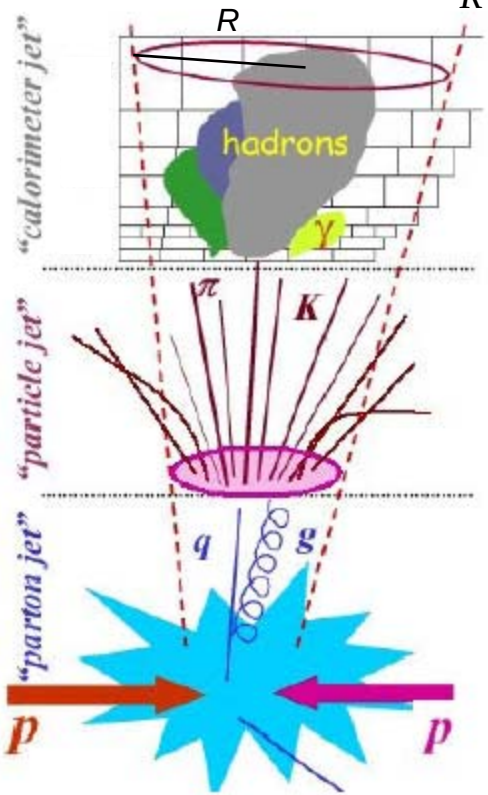

Calojets

Genjets

Partons

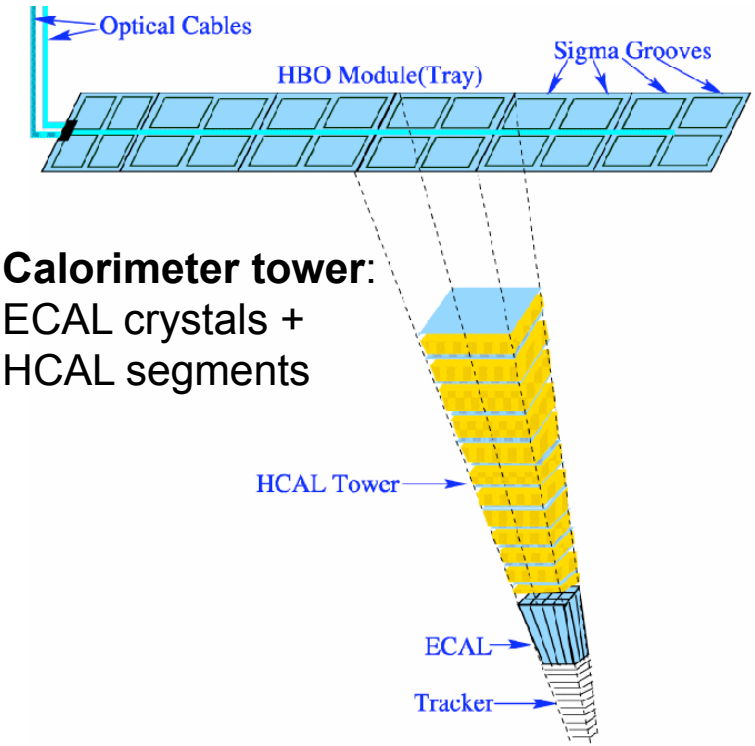

Calorimeter tower:
ECAL crystals +
HCAL segments

- **Coloured partons from the hard scatter evolve via soft quark and gluon radiation and hadronisation process to form a spray of roughly collinear colorless hadrons -> Jets**
- **Jets are the experimental signatures of quarks and gluons.**

Event selections – Detector Level (Calojets)

- Jets are selected in the $|\eta| < 3.0$ region (upto endcap).
- Jet algorithm used : Cone Algorithm with $\Delta R=0.5$.
- Jet Energy Corrections are applied on the Calorimeter jets.

- Events pass through HLT80 trigger bit + satisfy $MET/SumE_T < 0.3$.
- Offline selection: Leading Calojet p_T (corrected) > 110 GeV/c.

  All Calojet p_T (corrected) > 50 GeV/c.

Ratio of **HLT80/HLT50** for Leading jet p_T

- Estimation of the p_T threshold for the HLT trigger to be more than 99% efficient.

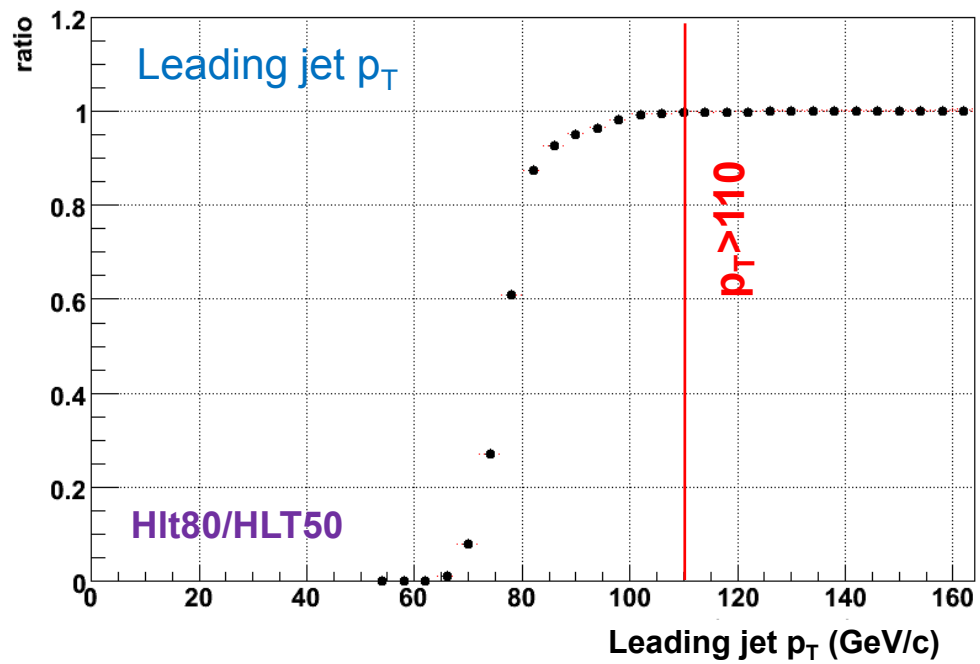

Event selections - TrackJets

❖ Track jets:

- The charged energy fraction in jets is about 60%.
- The charged tracks can be clearly associated to the interaction vertex and can define multi-jet shapes correctly even in an environment with pile-ups.
- Jet finding with charged tracks only is completely independent from jet finding with calorimeter towers and could prove to be a good way to complement the other.

ValidHits > 8

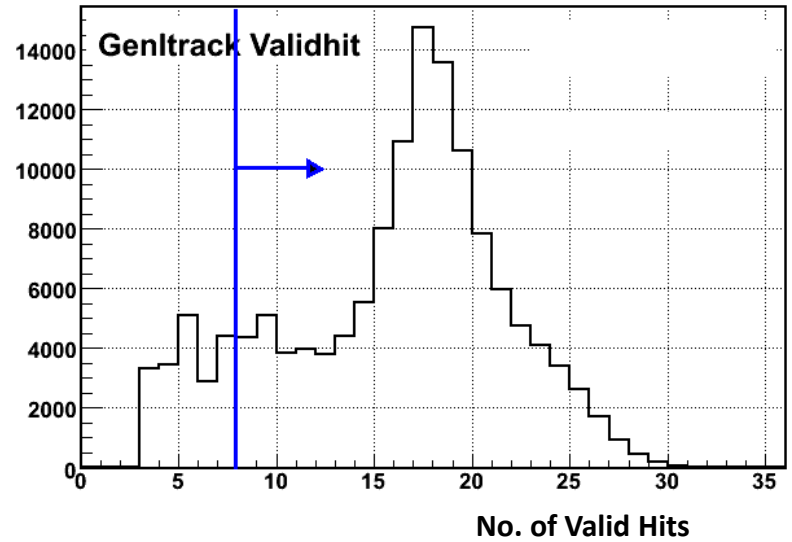

❑ Event selection:

- Events pass through HLT80 trigger.
- Tracks are selected in the $|\eta|<1.3$ region (upto barrel).
- Tracks are required to have
  - $p_T>0.9$ GeV/c
  - No. of Valid Hits > 8
- Offline threshold of 80 GeV/c on leading jet p_T on Trackjets.
- A min p_T threshold (25 GeV/c) is applied on all Trackjets.

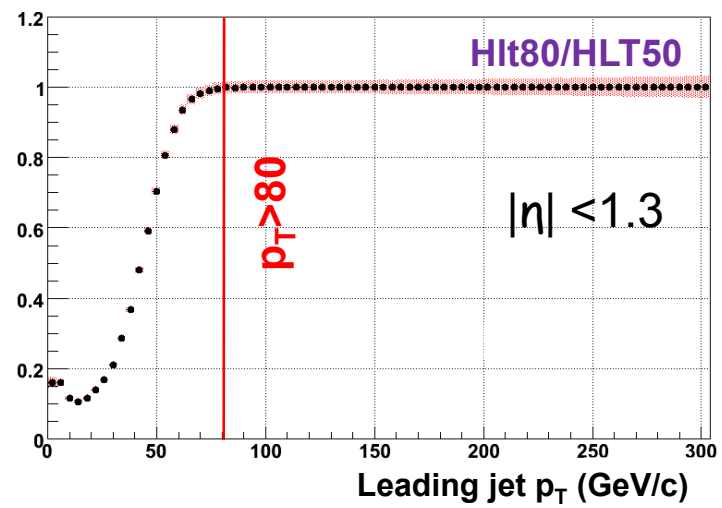

QCD studies in CMS with Multijets at $\sqrt{s}$=10 TeV

(CMS AN-2009/073)
CMS Approved

Motivation

- The essential features of QCD are provided by the vector nature of gluon and gluon self coupling (which is the nonabelian nature of QCD). These reflect on the so called color factors which appear in various vertices.

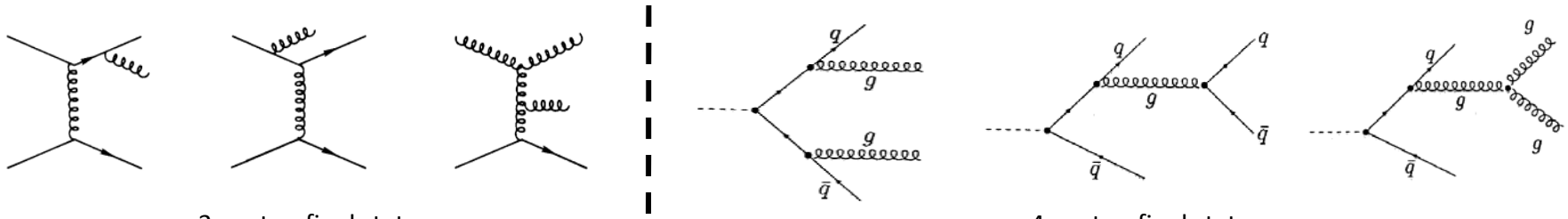

3-parton final states

4-parton final states

- Several tests of QCD which are sensitive to the gluon self-coupling have already been carried out in the earlier e^+e^- experiments which are based on study of angular correlations in 3-jet and 4-jet events.

- Study of multi-jet events allows a test of the validity of the QCD calculations to higher order and a probe of the underlying QCD dynamics. The topological distributions of these multijet events provide sensitive tests of the QCD matrix element calculations.

Topological properties of multi-jet events

$1+2 \rightarrow 3+4+5$

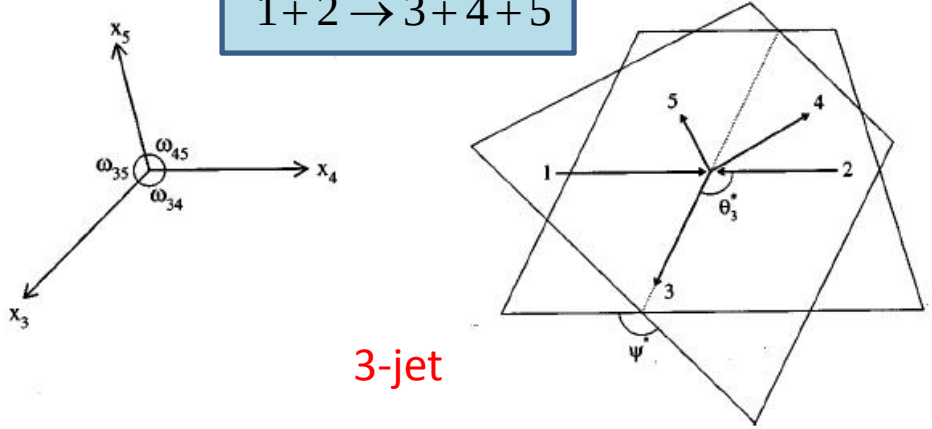

3-jet

- Scaled energies: ordered in their c.m. frame:

$$x_i = 2E_i / \sqrt{\hat{s}_{345}} \quad \text{where} \quad x_3 + x_4 + x_5 = 2$$

- Angles that fix the event orientation – Cosine of angle of parton 3 w.r.t beam ($\cos\theta_3$).

- Angle (Ψ) between the plane containing partons 1 and 3 and the plane containing partons 4 and 5 defined by

$$\cos\psi = \frac{(\vec{p}_1 \times \vec{p}_3)\cdot(\vec{p}_4 \times \vec{p}_5)}{|\vec{p}_1 \times \vec{p}_3||\vec{p}_4 \times \vec{p}_5|}$$

$1+2 \rightarrow 3+4+5+6$

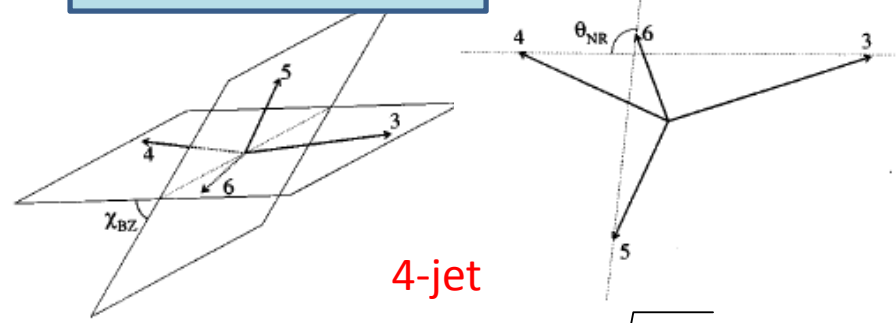

4-jet

- Scaled energies: $x_i = 2E_i / \sqrt{\hat{s}_{3456}}$
- Cosine of polar angles: $\cos\theta_i$
- **Bengtsson-Zerwas angle** :
  Angle between the plane containing the two leading jets and the plane containing the two non-leading jets.

$$\cos\chi_{BZ} = \frac{(\vec{p}_3 \times \vec{p}_4)\cdot(\vec{p}_5 \times \vec{p}_6)}{|\vec{p}_3 \times \vec{p}_4||\vec{p}_5 \times \vec{p}_6|}$$

- **Nachtmann-Reiter angle**:
  Angle between the momentum vector differences of the leading jets and the two non-leading jets:

$$\cos\theta_{NR} = \frac{(\vec{p}_3 - \vec{p}_4)\cdot(\vec{p}_5 - \vec{p}_6)}{|\vec{p}_3 - \vec{p}_4||\vec{p}_5 - \vec{p}_6|}$$

Invariant masses of 3 and 4 jet final states

- We use PYTHIA Monte Carlo samples for looking into multi-jet final states.
- Inclusive 3 jet and 4 jet events selected.
- For 3(4) jet studies the most energetic jets are considered, the jets being ordered in their transverse momentum (p_T).
- The jets are boosted to the 3(4) jet centre of mass frame and ordered in descending order of their Energies (E) in the boosted frame.

❑ Expected distributions are estimated at an integrated luminosity of 10 pb^{-1}.

❑ Effect of hadronisation is different for different multijet variables. Hence several variables need to be examined for a better understanding of the underlying nature of the fundamental processes.

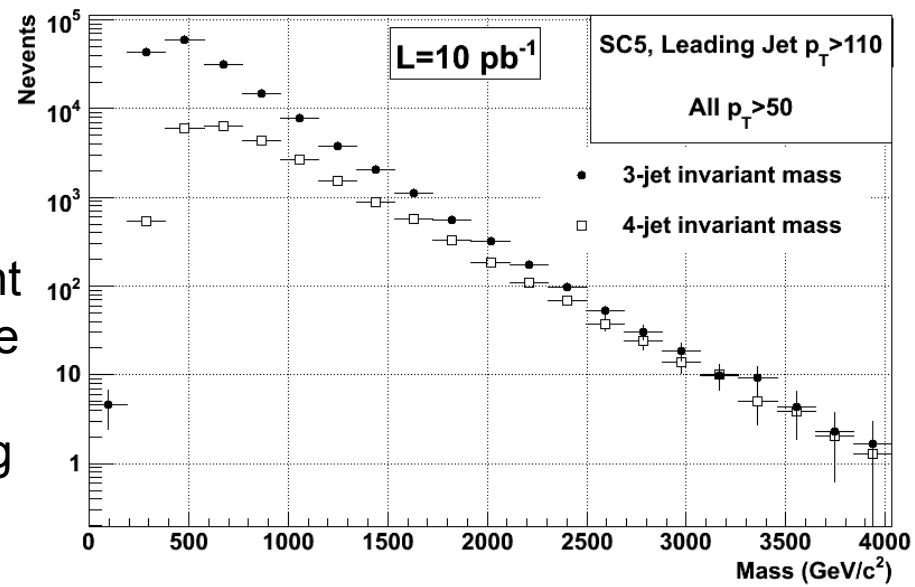

❖ Invariant masses ($\sqrt{\hat{s}}$) for 3jet and 4jet final states.

Effect of Angular Ordering

- **Angular Ordering (AO)** is an important consequence of colour coherence.
- It results in <u>suppression of soft gluon radiation</u> in partonic cascade in certain regions of phase space.
- For outgoing partons AO requires that the emission angles of soft gluons decrease monotonically as the partonic cascade evolves away from the hard process.
- PYTHIA incorporates colour coherence effects by means of AO approximation of parton cascades.

o **AO constraint is turned off and distributions are compared with default PYTHIA.**

✓ **Difference within 6% which is comparable statistical errors.**

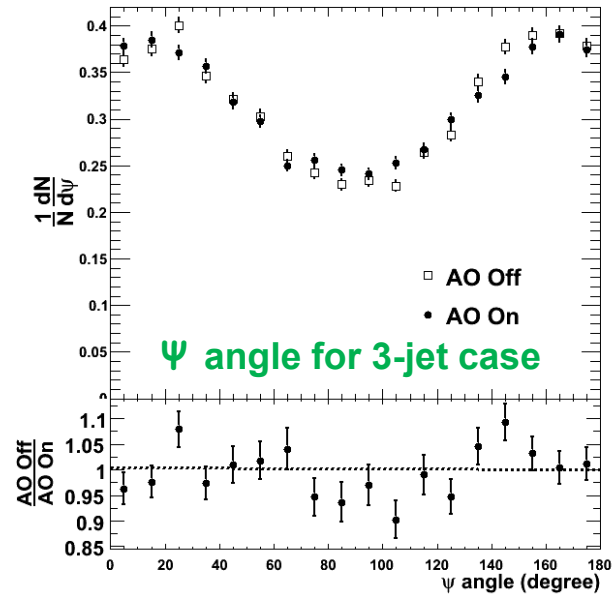

4%

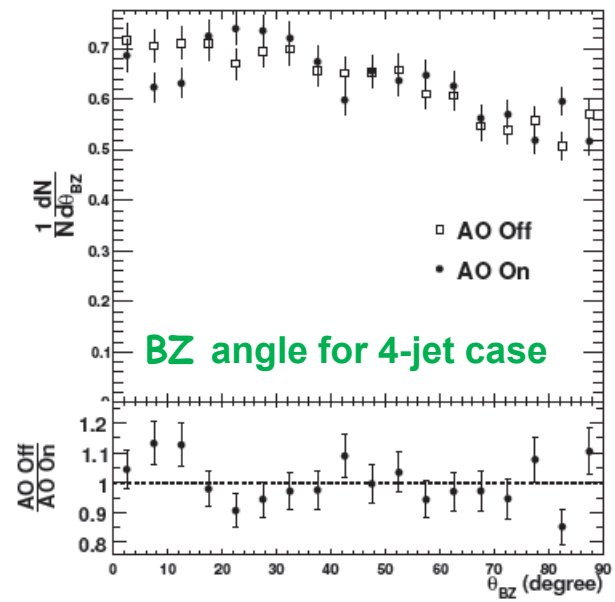

6%

Detector effects

- Detector effects such as the jet energy and position resolution can affect the multi-jet distributions.

- A closer look to see the source of detector corrections:
  - Energy resolution
  - Position resolution
    -- Effect on η, ϕ

- Resolutions on these quantities are obtained by studying the bulk properties of Monte Carlo jets using full simulation.

- For each event, all generated jets are smeared in p_T / η / ϕ, depending on the effect that is tested, using the corresponding jet resolution function derived from Monte Carlo. A Gaussian distribution is considered during the smearing process.

- The smeared collection is reordered in p_T and new multi-jet distributions are calculated.

- The effects are estimated by taking the ratio between the new distributions and the ones from the original generated jet collection.

Detector effects : 3-jet properties

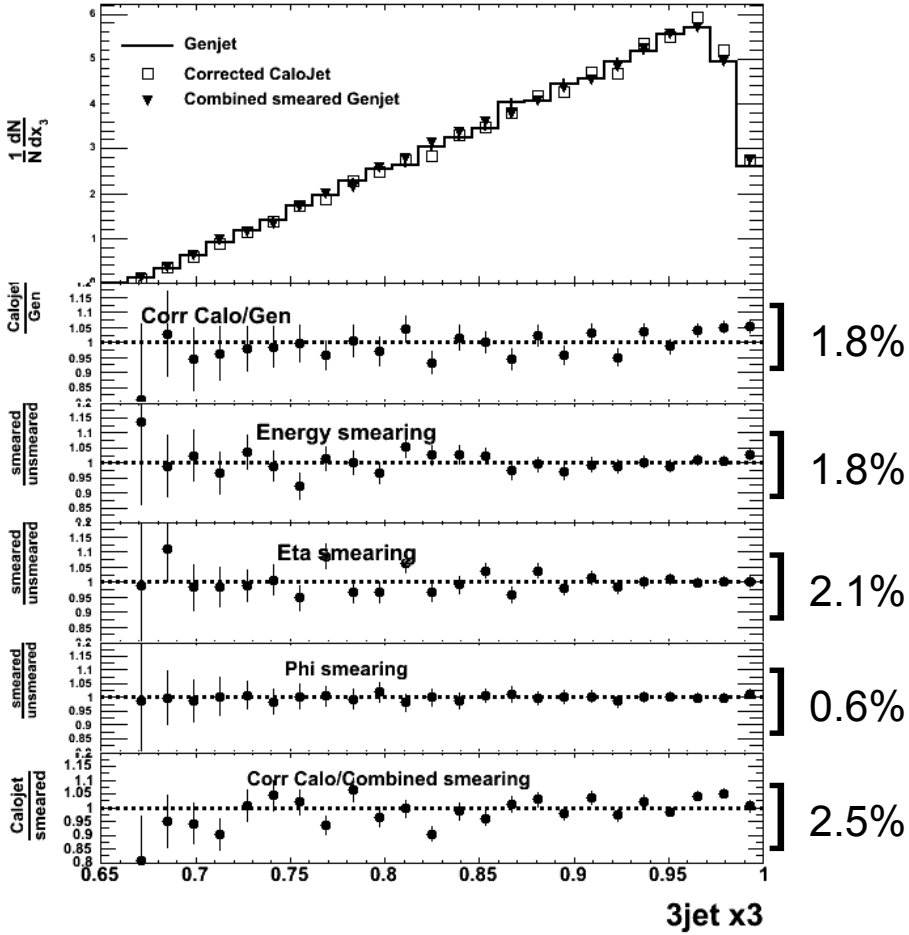

3-jet: scaled energy for hardest jet

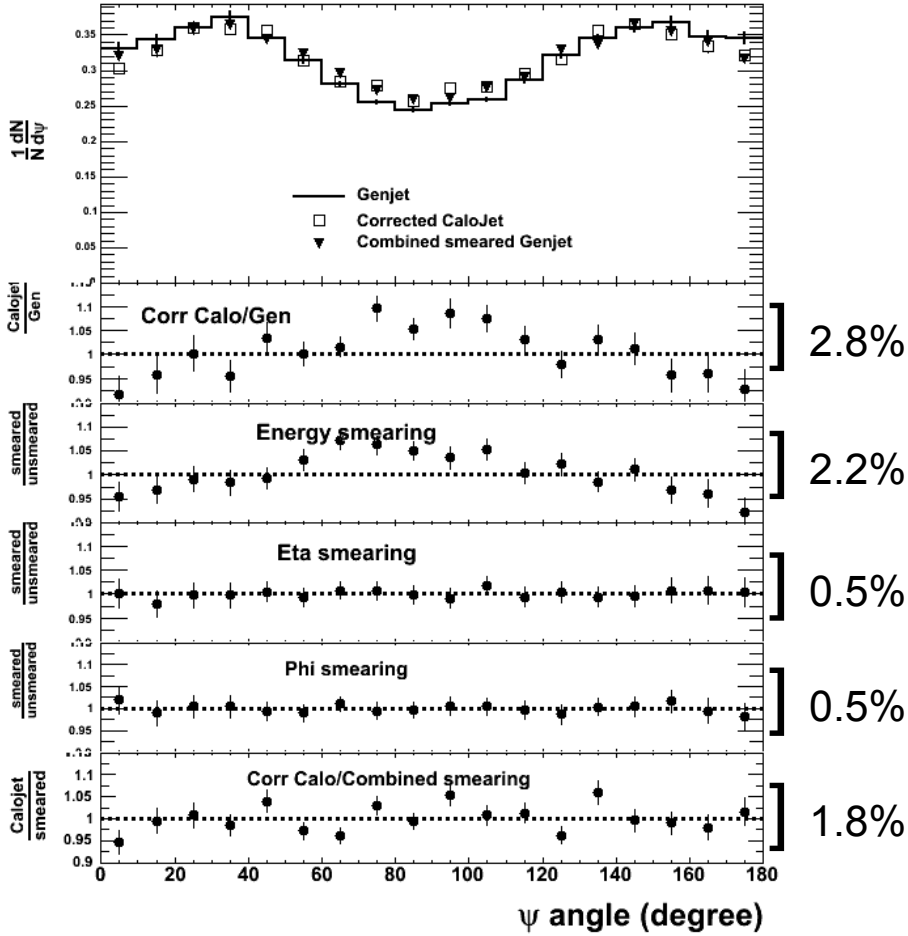

3jet : Angle between jet planes

- Scaled energies are less sensitive to detector effects than the angular variables.
- Combined smearing partially reproduces detector effects.

Detector effects : 4-jet properties

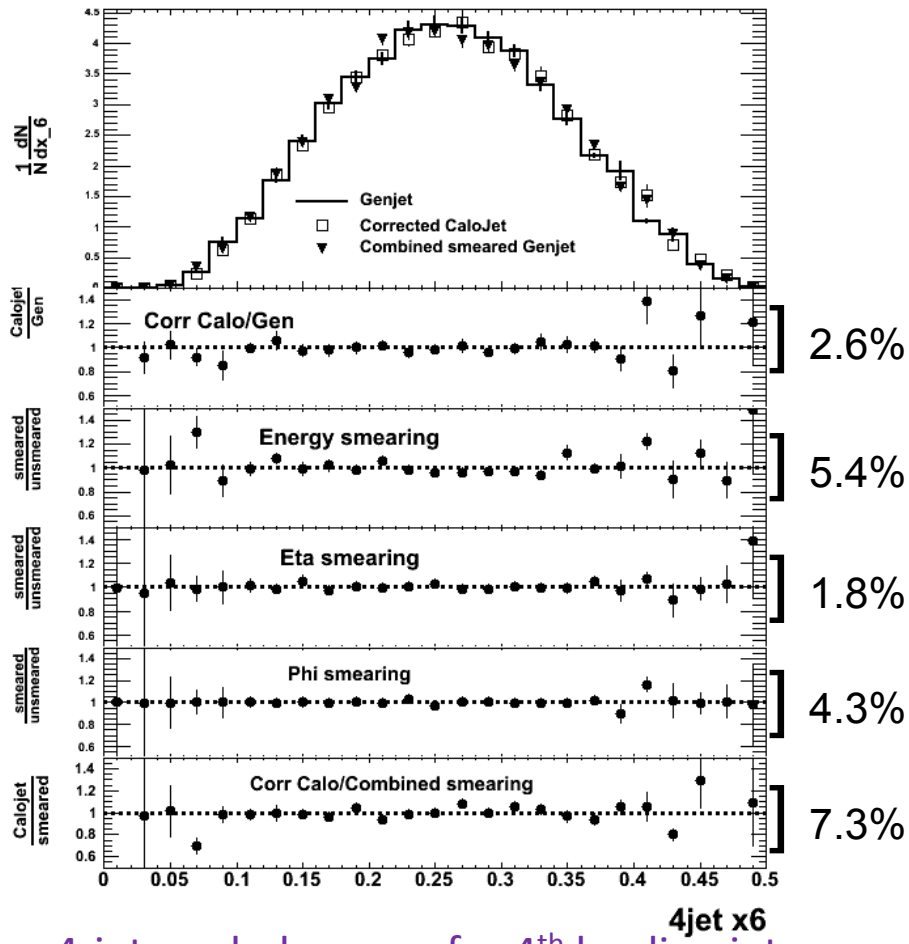

4-jet: scaled energy for 4th leading jet

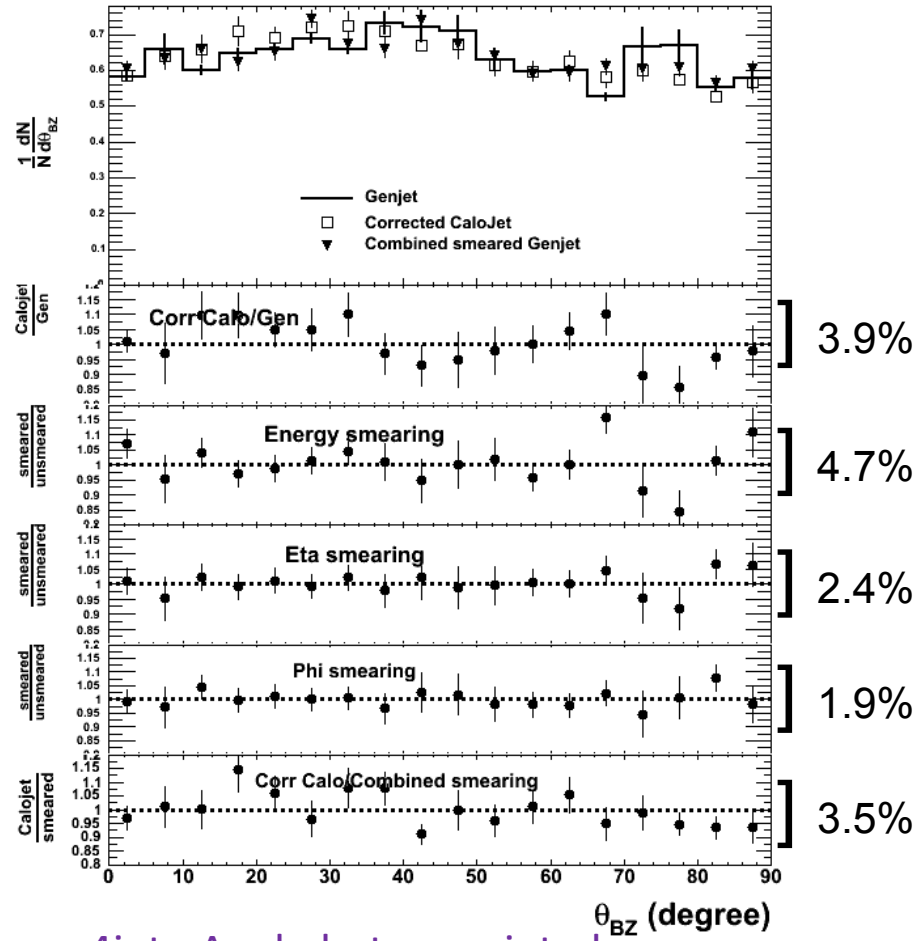

4jet : Angle between jet planes

❖ The small residual difference between the detector level distributions and the generator level ones with smearing are assigned as systematic uncertainty for the unfolding detector correction.

Systematic effects: Jet Energy Scale

- We assume a global uncertainty of 10% on the knowledge of the jet energy scale.
- Vary jet p_T by ±10% and measure uncertainty in the distributions.
- Uncertainties due to jet energy scale are tabulated below for some variables.

Variable	Average Uncertainty (RMS in %)
3jet x3	2.2
4jet x6	3.9
3jet Ψ	1.0
4jet θ_{BZ}	2.4

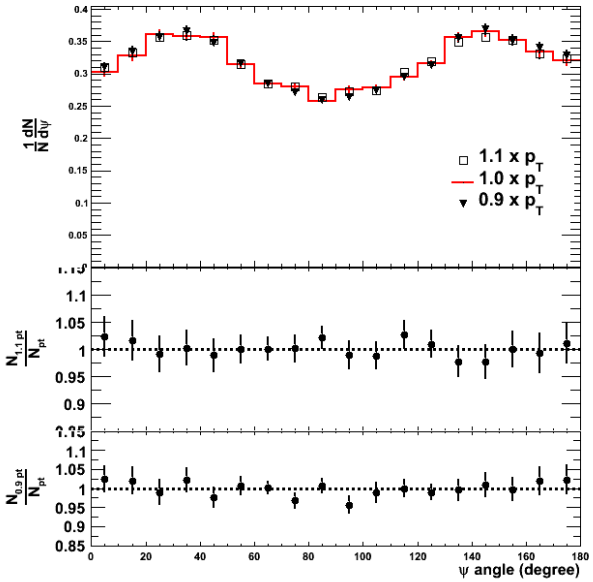

Ψ angle for 3-jet case

0.9%

1.1%

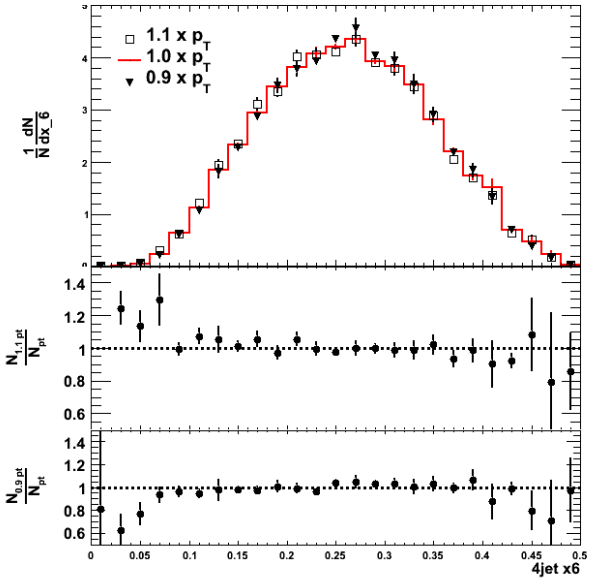

Scaled energy of the 4th jet

3.0%

4.6%

Matrix Element vs. Parton Shower

- Matrix element generation on N partons (N=2,3,≥4) with MadGraph, p_T > 20 GeV.
- Showering by PYTHIA
- Combination (MadGraph + PYTHIA) using MLM matching.

✓ There is a significant difference in the distribution for harder jets (~17%) between PYTHIA and Madgraph but for softer jets the agreement is within 9%.

✓ The angular variables (θ_{BZ} and $\cos\theta_{NR}$) match within 4% between PYTHIA and Madgraph.

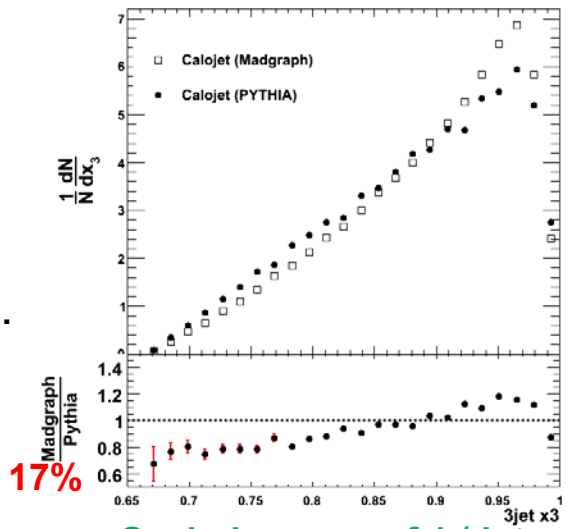

17%

Scaled energy of 1st jet

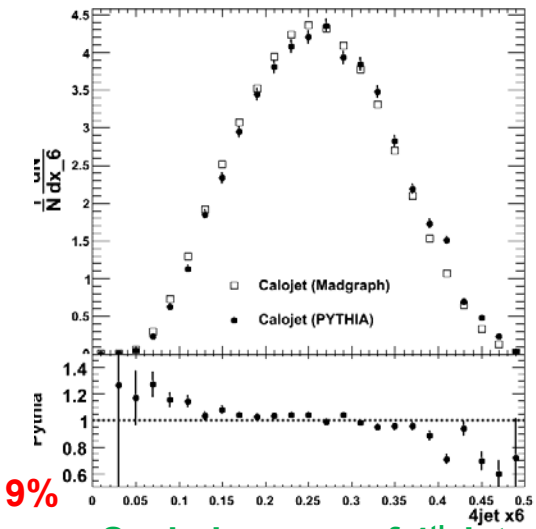

9%

Scaled energy of 4th jet

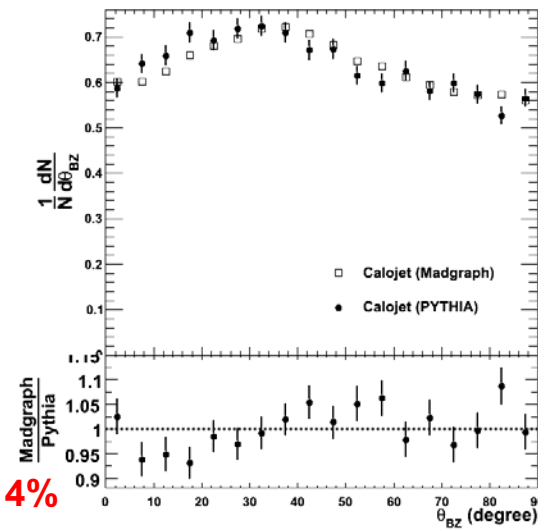

4%

BZ angle for 4-jet case

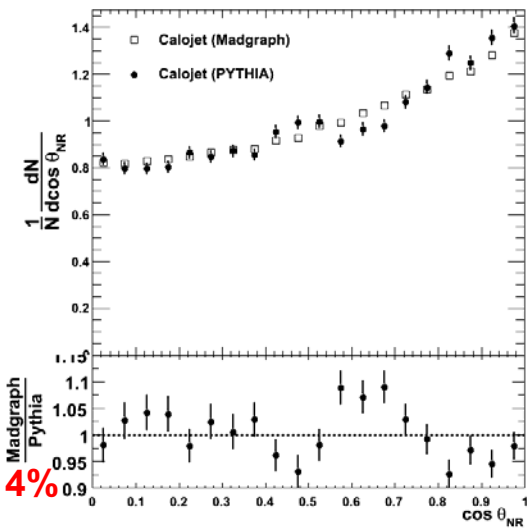

4%

NR angle for 4-jet case

PYTHIA vs. HERWIG

- Fragmentation and hadronisation are treated differently in PYTHIA and HERWIG + JIMMY.

PYTHIA → String model

HERWIG → Cluster model

- Multi-particle interaction also treated differently in the two models.

✓ There is significant difference in the distributions for scaled energies (~15%) between PYTHIA and HERWIG.

✓ For angular variables the differences are within 5%.

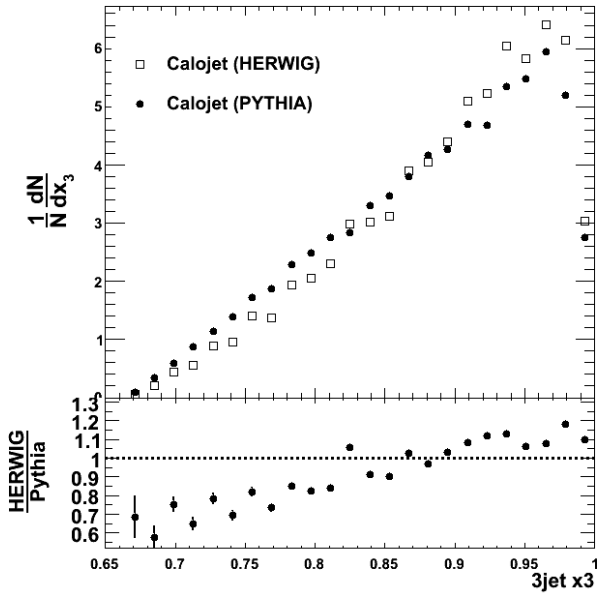

Scaled energy of 1st jet

15%

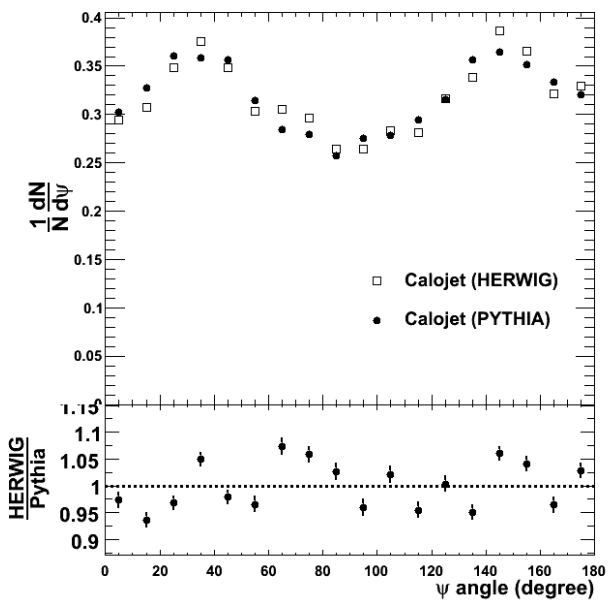

Ψ angle for 3-jet case

5%

Final Comparisons

- Distributions as expected to be measured at L=10pb^{-1} data are unfolded back to particle level using PYTHIA Monte Carlo. The unfolded distributions are compared with predictions from different generators at particle level.

- The uncertainty due to unsmearing are added in quadrature with the jet energy scale uncertainty.

- Total uncertainty = Statistical $\oplus$ Systematic (from JES $\oplus$ Unsmearing)

- The distributions with total uncertainty are compared with event generator models: PYTHIA, HERWIG(+Jimmy), MADGRAPH

Final Results: 3-jet variables

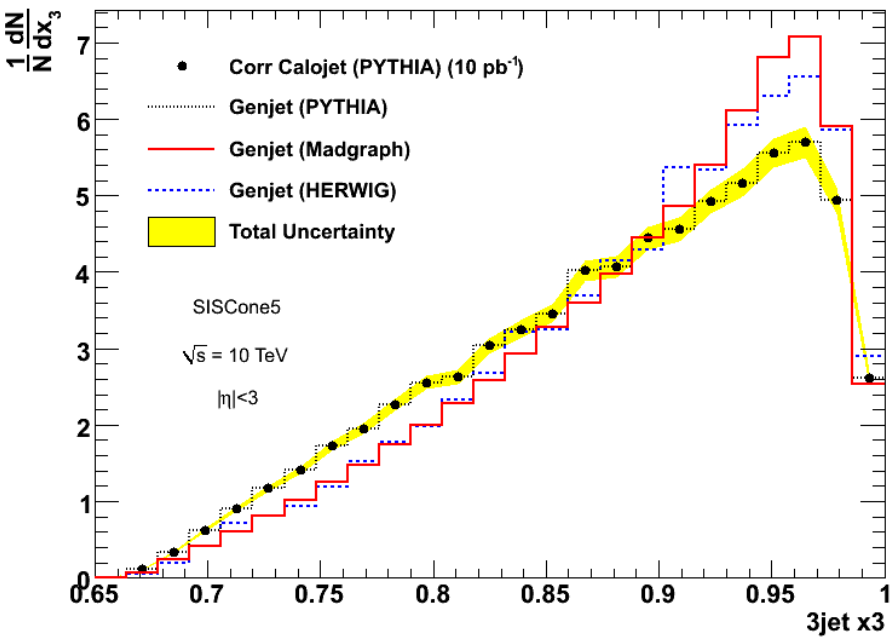

Scaled energy of leading jet

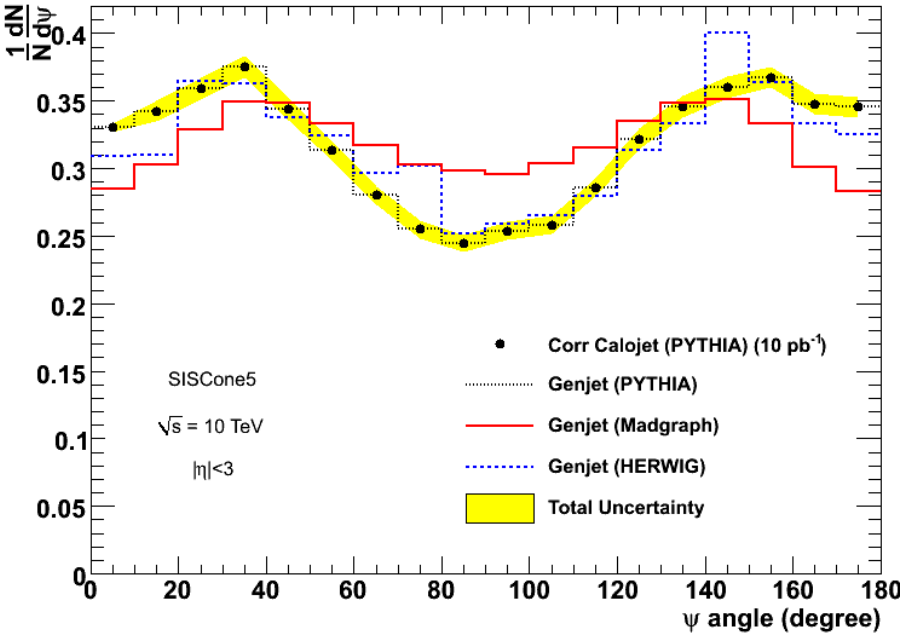

Ψ angle for 3-jet case

- Expected distributions with the total uncertainty have sensitivity to distinguish among different event generators - PYTHIA, Herwig+Jimmy, MADGRAPH.
- Discrepancies between the generators are larger than expected systematic uncertainties.

Final Results: Angular variables of 4jets

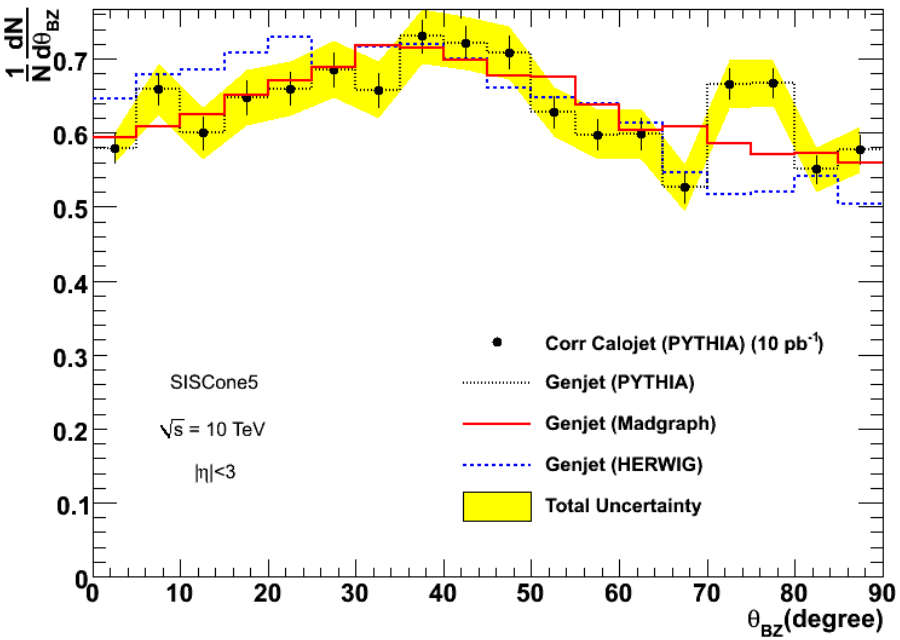

BZ angle for 4-jet case

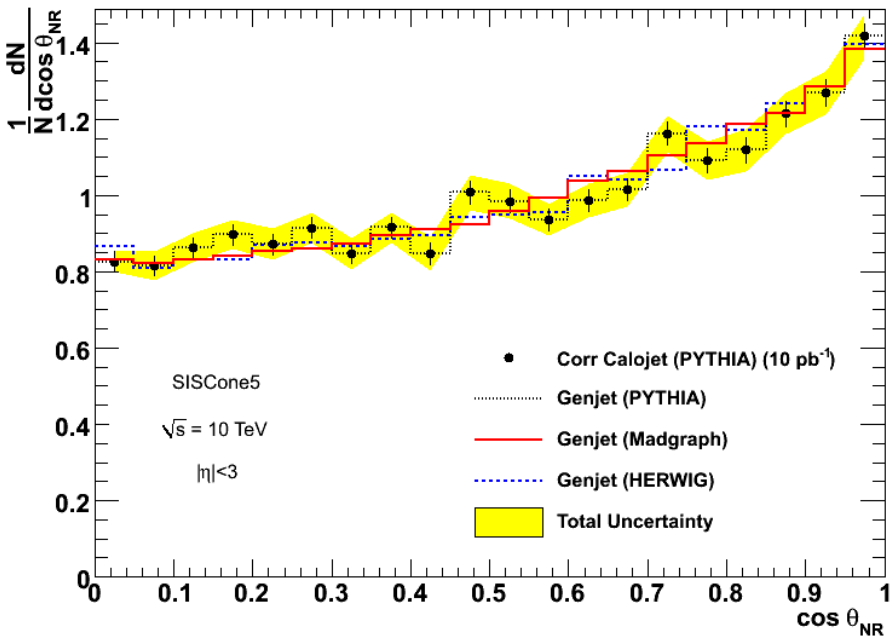

NR angle for 4-jet case

- Expected distributions with the total uncertainty can not distinguish among different event generators for these angular variables.
- Small discrepancies observed among the three generators.

Study of Event Shape Variables in CMS at $\sqrt{s}$=10 TeV

Event Shape Variables

❑ Event shape variables, constructed from linear sums of measured particle momenta, are sensitive to the amount of hard gluon radiation and offer a way to measure α_s in hadron collisions. One such variable, **Thrust**, *defined as:*

$$T = \max_{\hat{n}_T}\left(\frac{\sum_i |\, p_i \cdot \hat{n}_T \,|}{\sum_i |\, p_i \,|}\right)$$

Where thrust axis n_T is defined as the unit vector n, which maximises the expression.

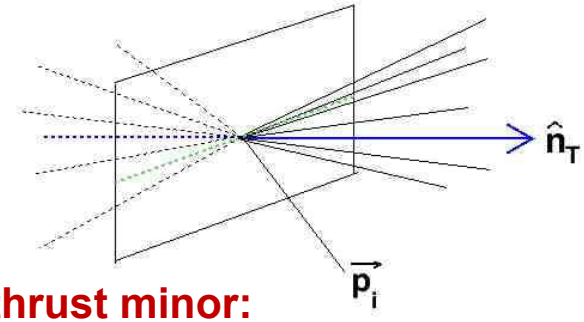

- **Central transverse thrust:**

$$T_{\perp,C} = \max_{\vec{n}_T} \frac{\sum_{i\in C} |\, \vec{p}_{\perp,i} \cdot \vec{n}_T \,|}{\sum_{i\in C} \vec{p}_{\perp,i}}$$

- **Central transverse thrust minor:**

$$T_{m,\mathcal{C}} \equiv \frac{\sum_{i\in\mathcal{C}} |p_{x,i}|}{\sum_{i\in\mathcal{C}} p_{\perp,i}} = \frac{\sum_{i\in\mathcal{C}} |(\vec{p}\times\vec{n}_B)\times\vec{n}_{T,\mathcal{C}}|}{\sum_{i\in\mathcal{C}} p_{\perp,i}}$$

- **Jet Broadenings:**
- Split events into two hemispheres (C_U, C_D) divided by a plane orthogonal to thrust axis

$$B_{\pm,C} = \frac{\sum_{i\in S_\pm} |\, \vec{p}_{\perp,i} \times \vec{n}_{T,C} \,|}{2\sum_i |\, \vec{p}_{\perp,i} \,|}$$

where C_U: $\vec{p}_\perp \cdot \vec{n}_{T,\mathcal{C}} > 0$ and C_D: $\vec{p}_\perp \cdot \vec{n}_{T,\mathcal{C}} < 0$

- Central wide Jet Broadening: $B_{W,C} = \max(B_{+,C}, B_{-,C})$
- Central total Jet Broadening: $B_{T,C} = B_{+,C} + B_{-,C}$

Global Event Shape Variables

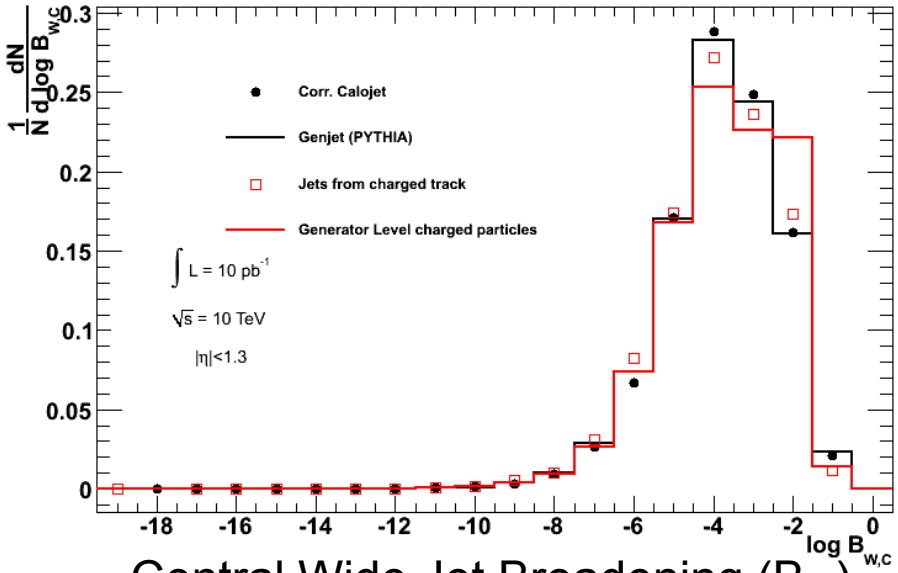

Central Wide Jet Broadening (B_W)

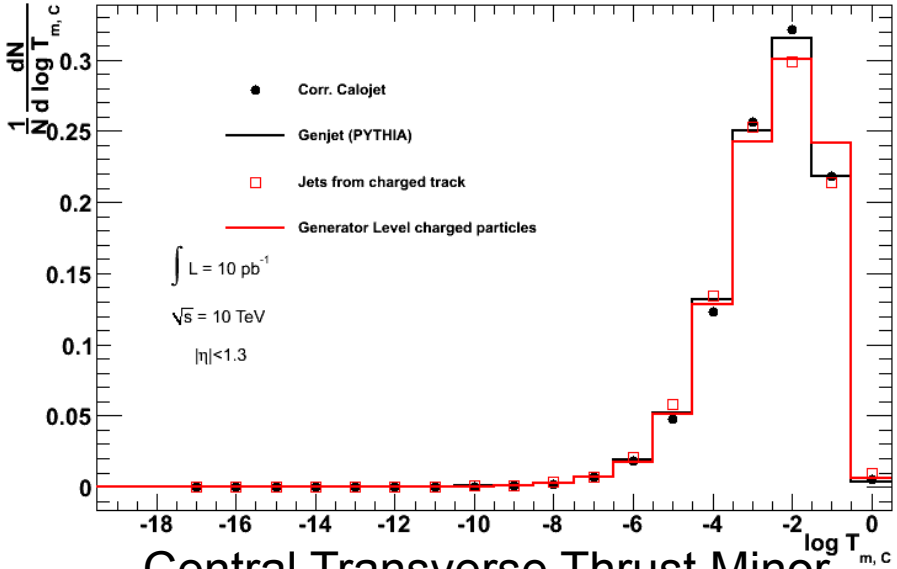

Central Transverse Thrust Minor

Comparisons among:

Particle level	**Detector Level**
GenJet (PYTHIA)	**Corr. CaloJet (PYTHIA)**
Charged particles	**Jets from charged tracks**

- We have reasonable agreement in distributions from calorimetric jets and track jets.

Event Shape: Central Transverse Thrust

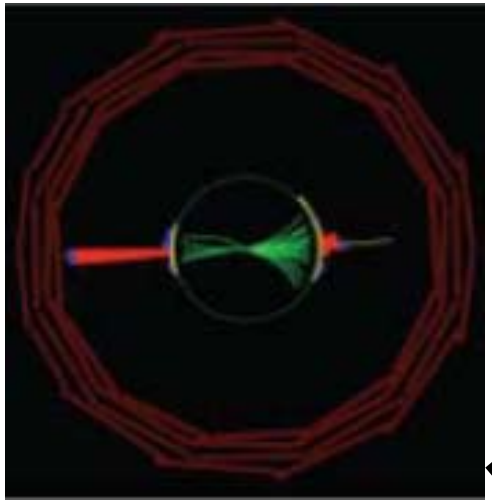

$\tau_{\perp,C}=0$

$$\log \tau_{\perp,\mathcal{C}} = \log(1 - T_{\perp,\mathcal{C}})$$

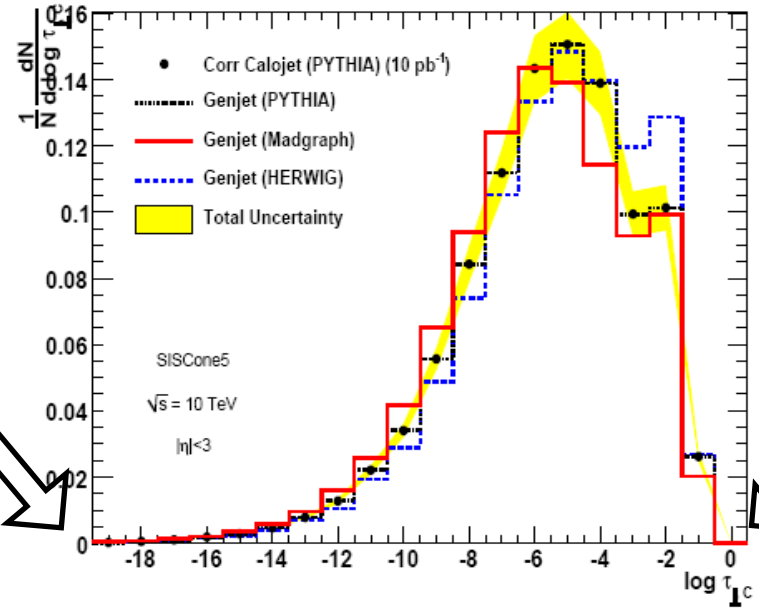

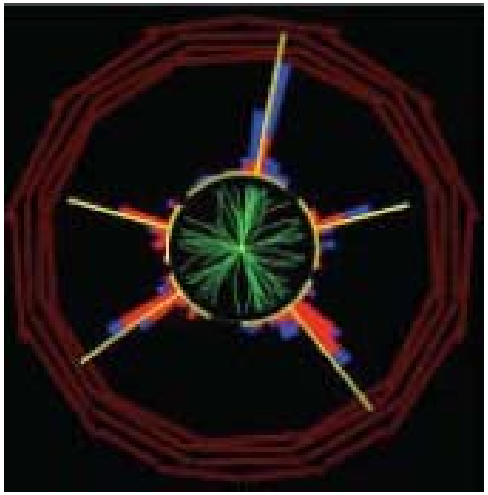

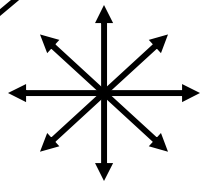

$\tau_{\perp,C} = 1/2$

Expected distributions for transverse thrust with the total uncertainty are compared with different event generators - PYTHIA, Herwig+Jimmy, MADGRAPH.
Total uncertainty = Statistical $\oplus$ Systematic (from JES $\oplus$ Unsmearing)

Distinguishing capability among different event generators.

Summary

- Single particle response and resolution of CMS calorimeter system is studied for the endcap.
- Different topological variables for inclusive 3-jet and 4-jet events are studied with calorimeter jets.
- Different event generator models are compared. Matrix element calculation such as MADGRAPH are compared with parton shower models such as PYTHIA and HERWIG.
- Global event shape variables are studied. Comparisons were made with jets at the detector level and at the particle level.

BACK UP SLIDES

CMS Calorimeter System

CMS calorimeter (ECAL+HCAL) – Very hermetic (no projective gap)

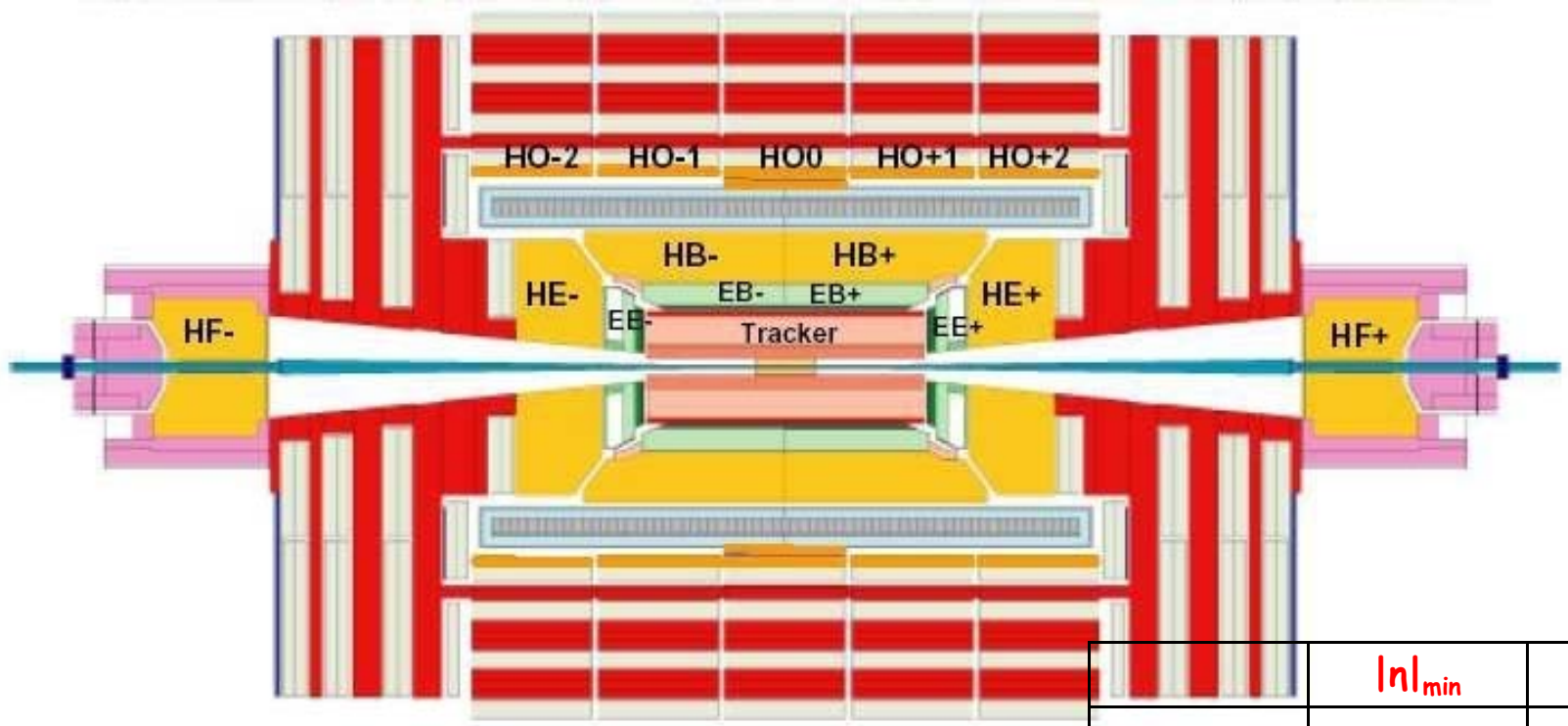

HB/ HE/ HO:
Brass absorber +
Scintillator Tile
Photo Detector (HPD)
HF: Steel absorber +
Quartz fibers
Photo Detector (PMT)

EB/EE:
PbWO4 crystals
Photo Detector:
APD (EB) / VPT(EE)
ES: Lead absorber +
silicon sensors

	$\lvert\eta\rvert_{min}$	$\lvert\eta\rvert_{max}$
HB	0.000	1.393
HE	1.305	3.000
HO	0.000	1.26
HF	2.853	5.191
EB	0.000	1.479
EE	1.479	3.000
ES	1.6	2.6

Calorimeter geometry of CMS

Granularity

$\Delta\eta \times \Delta\Phi = 0.0175 \times 0.0175$

Pb-Si Pre-shower

Crystals are projective and positioned pointing 3 degree off the IP to avoid cracks.

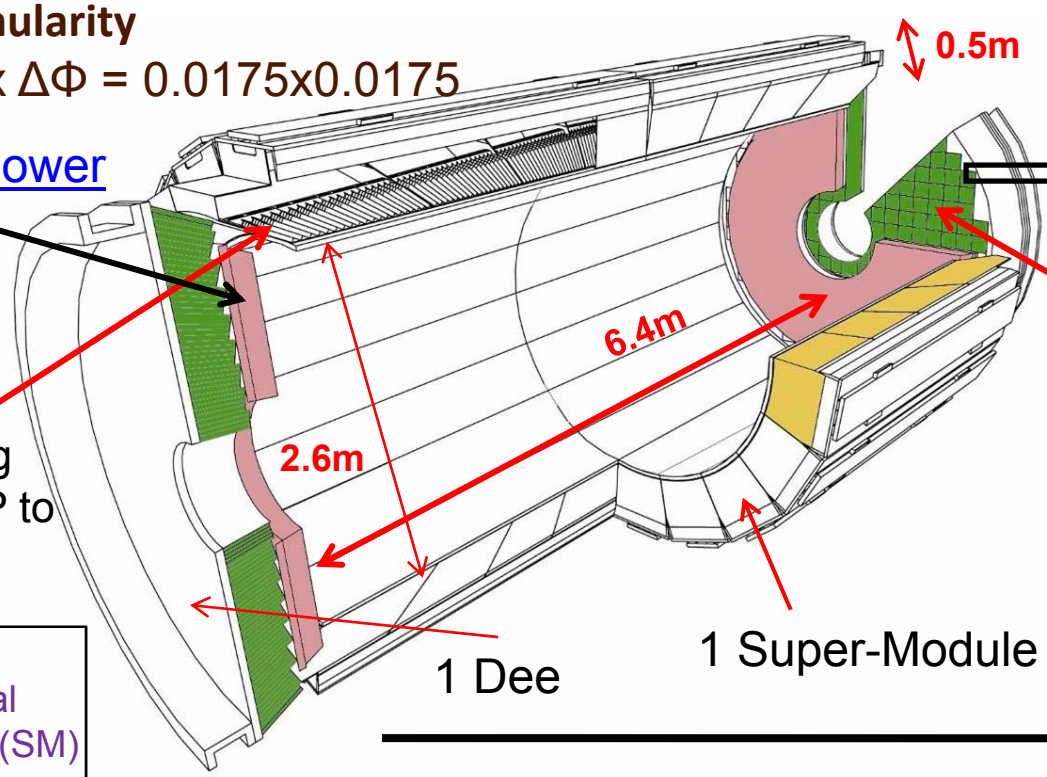

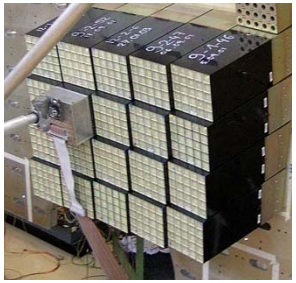

1 Endcap Super-Crystal

Endcap (EE):
- 4 Dees, each 3662 crystals
- Crystals combined into SuperCrystals of 5x5 crystals

Barrel (EB):
- 61200 crystals total
- 36 Supermodules (SM) each 1.7k crystals

- Thickness : 5.8 λ_I at $\eta = 0$
- Transverse granularity
  $\Delta\eta \times \Delta\varphi = 0.087 \times 0.087$ (in barrel)
- Two depths in barrel (HB, HO)
- 2/3 depths in endcap

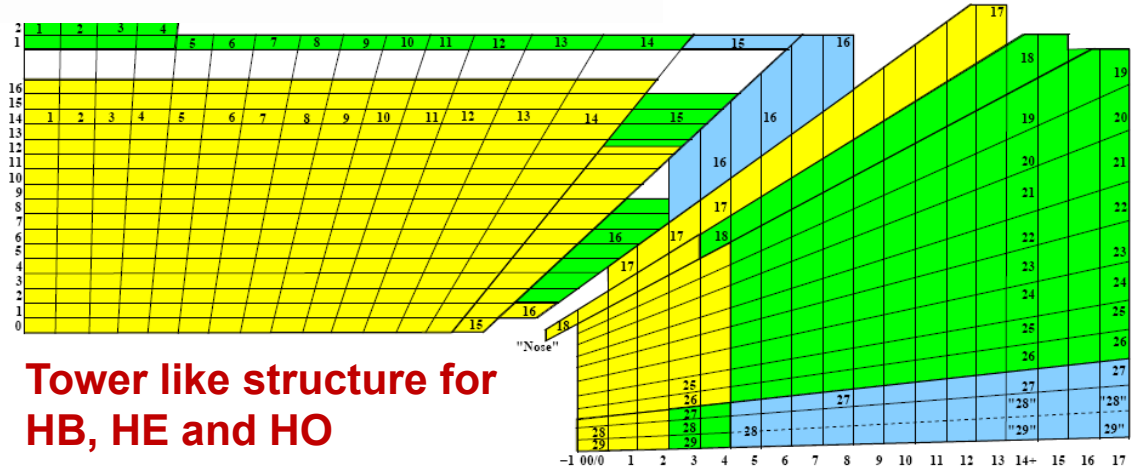

Tower like structure for HB, HE and HO

Digitisation of signal

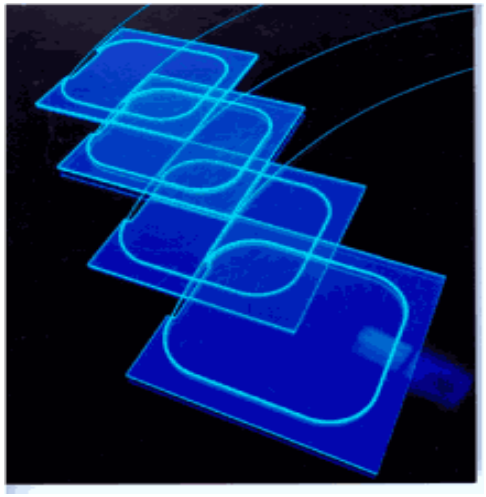

Scintillator tiles

- The optical signal in HCAL scintillator is collected using optical fibres and is converted to electronic signal using Hybrid Photodiodes.
- The analog signal obtained from the HPDs is spread over nearly 100 ns.

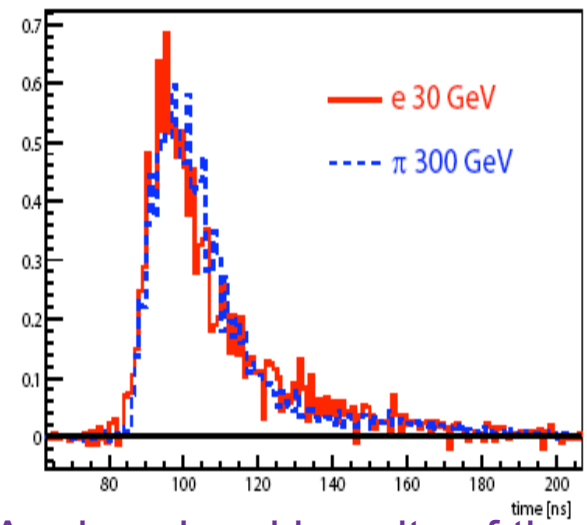

Analog signal in units of time

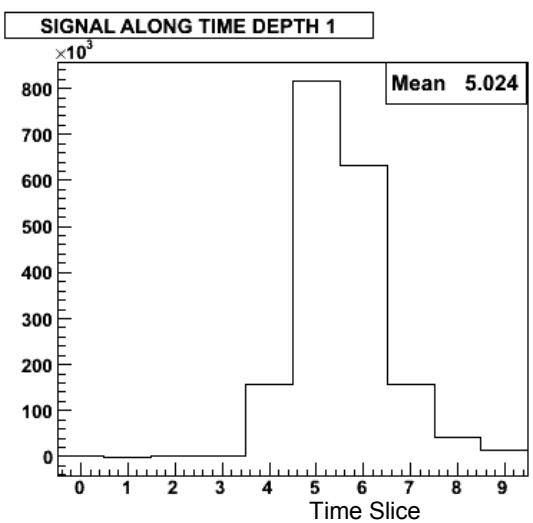

HE pulse shape

- The signal is digitized using an analog-to-digital converter Charge(Q) Integrator(I) and Encoder(E) in the bins of 25 ns (Time slice).
- More than 90% of the signal is usually contained in the sum of two time slices.
- Charge contained in 6 time slices is used in the test beam data analysis.

Calibration of HCAL channels

- The variation in signal produced can come from
  - the tile-to-tile variation in the amount of scintillation light produced,
  - the light transported by WLS fibres,
  - number of photo-electrons produced at HPDs.

- Inter-calibration of channels is done using Radioactive Source (Co^{60}).
- Determination of absolute energy scale is done using 50 GeV/c electron beam.

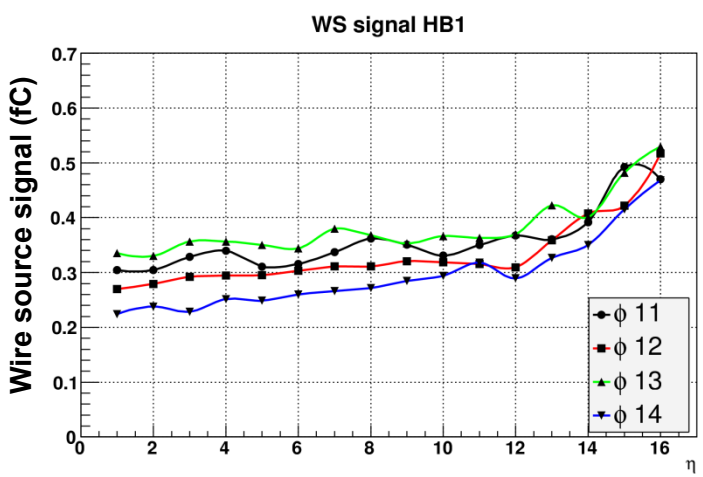

Relative calibration of Hcal channels in η index and ϕ index as in test beam.

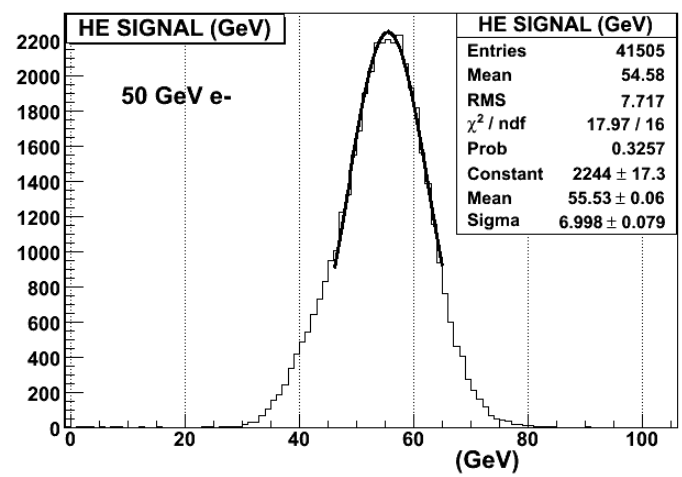

Scaling HE using 50 GeV e- beam.

Jet Algorithm Definitions

Official Jet Algorithms @ CMS

1. Seedless Infrared Safe Cone(SISCone)

- Searches for ALL stables cones
- Applies Split and Merge procedure
- Infrared and collinear safe.
- Fixed size cone of radius R=0.5, 0.7.

$$R = \sqrt{(\Delta\eta)^2 + (\Delta\varphi)^2}$$

2. k_T

- Successive recombination scheme
- Combines 4-vectors according to their relative Transverse momentum:

$$d_i = p_{T,i}^2$$

$$d_{ij} = \min(p_{T,i}^2, p_{T,j}^2)\frac{\Delta R_{ij}^2}{D^2}$$

- Infrared and collinear safe.

The jet algorithms take as input a set of 4-vectors:

1. GenJets
Stable simulated particles (after hadronization and before interaction with the detector)

2. CaloJets
Calorimeter energy depositions

3. TrackJets
Jet from Tracks

4. PFJets
Jets from particle flow

Particles, CaloTowers, PF, Tracks → **Jet Algorithms** → GenJets, CaloJets, PFJets, TrackJets

Jet energy scale corrections

The CMS calorimeter is not linear and non uniform. The measured jet energy needs to be corrected.

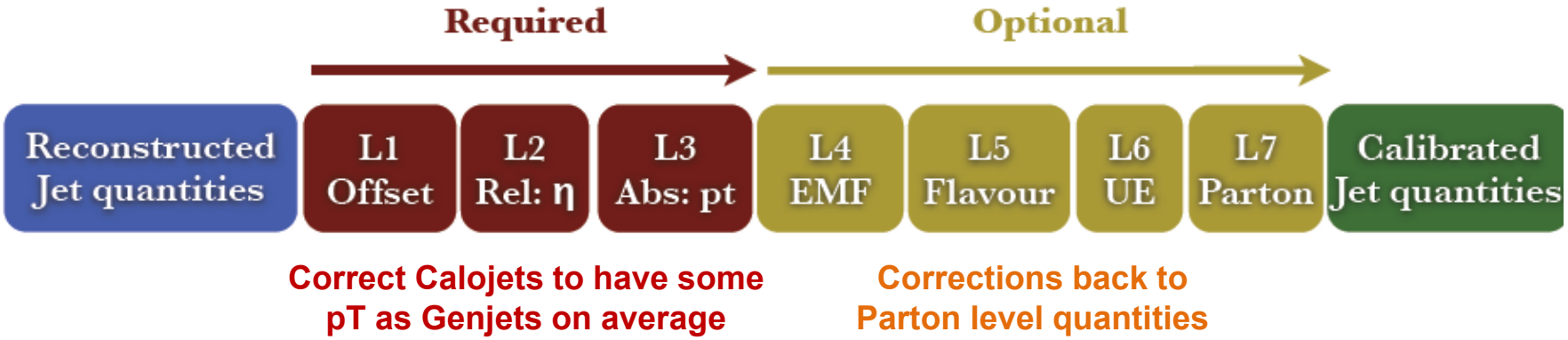

- **Offset:** correct for Pile Up and electronic noise in the detector (measure in zero-bias data)
- **Relative(η):** variations in jet response with η relative to a control region.
- **Absolute (p_T):** correcting the p_T of a measured jet to particle level jet versus jet p_T

Relative Jet Response vs. η

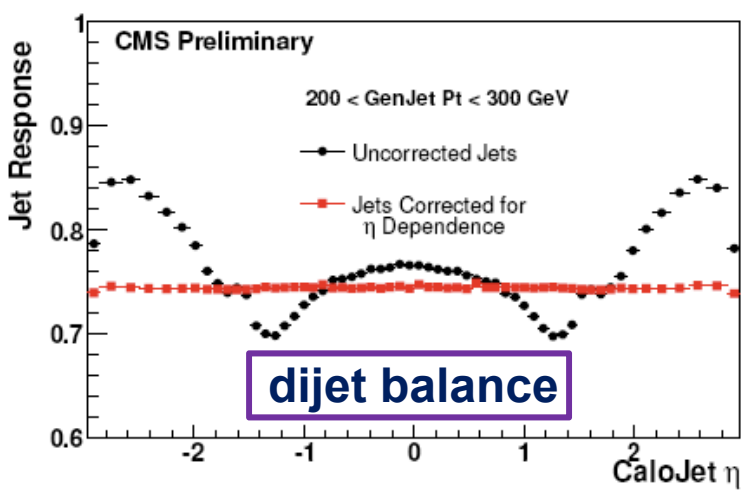

Jet Response vs. p_T

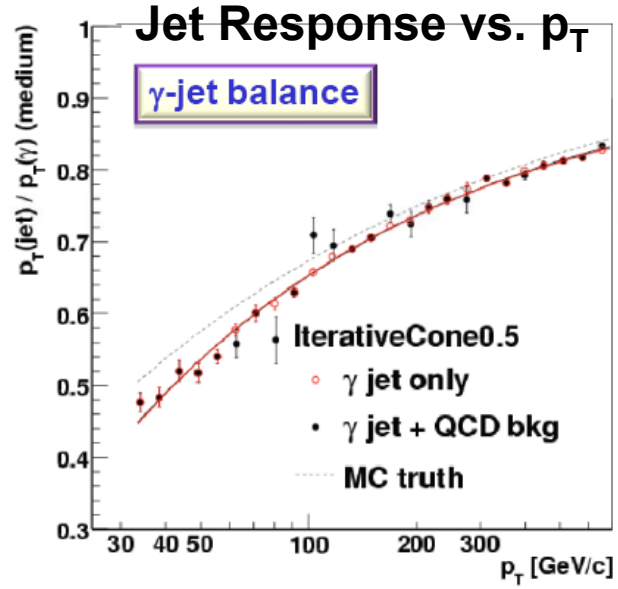

CERN Accelerator Complex

- A Proton Source
- Radio Freq Quadrupole (750 keV)
- LINAC2 (50 MeV)
- PS Booster (1.4 GeV) [170 m]
- PS (25 GeV) [621 m]
- SPS (450 GeV) [7 km]
- LHC (7 TeV) [27 km]

LHC beam crossing angle 300 μrad

Vacuum pressure inside beam pipe 10^{-8} torr

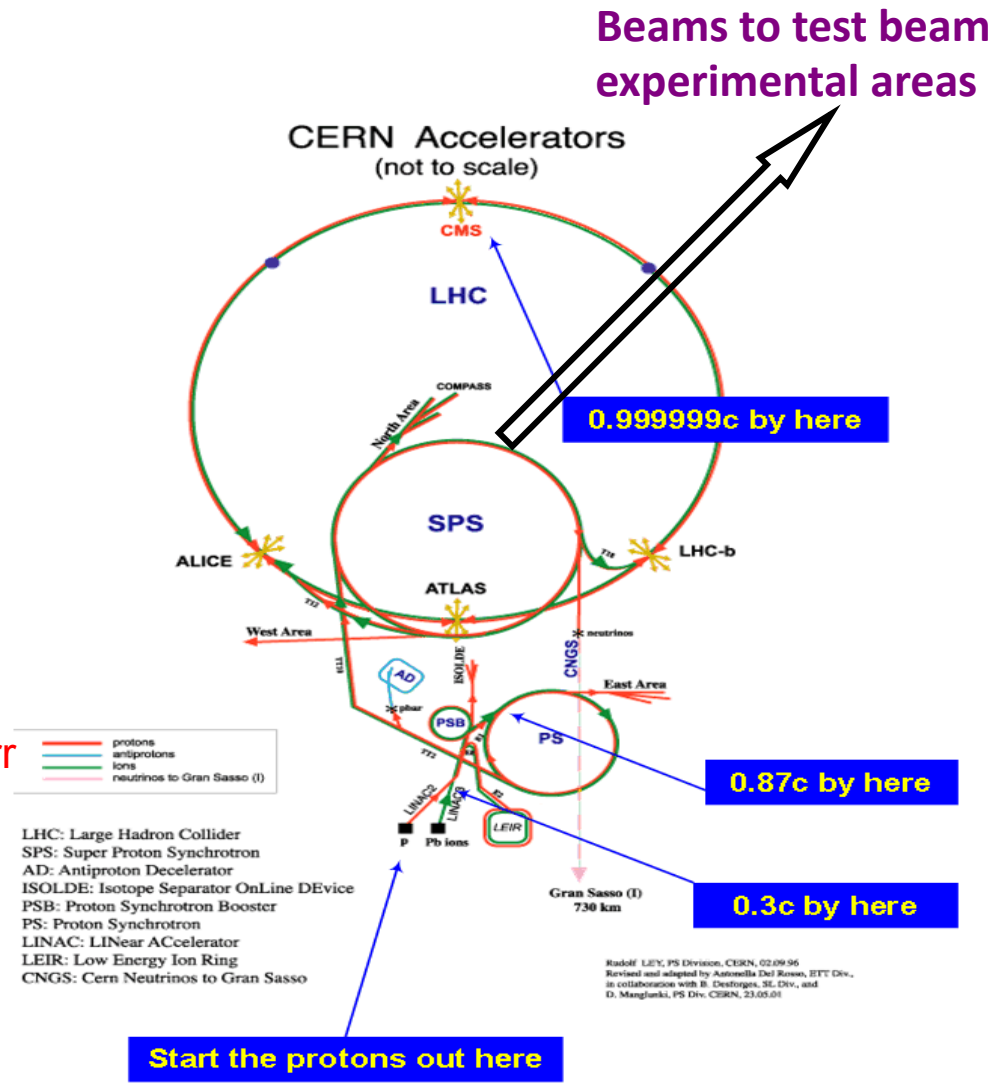

- Using 400 GeV Protons from SPS, derive secondary beams of hadrons in momentum range 2-300 GeV/c

Resolution in CMS vs. ATLAS

ATLAS and CMS Detectors

B field:	2.6 T (Solenoid), 4 T (Toroid)	3.8 T (Solenoid)

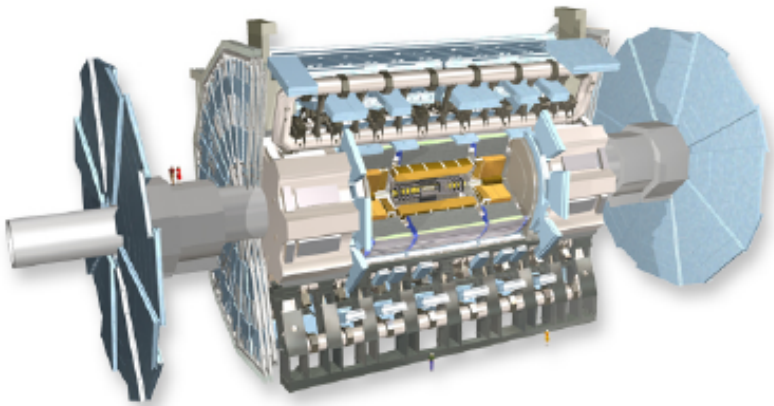

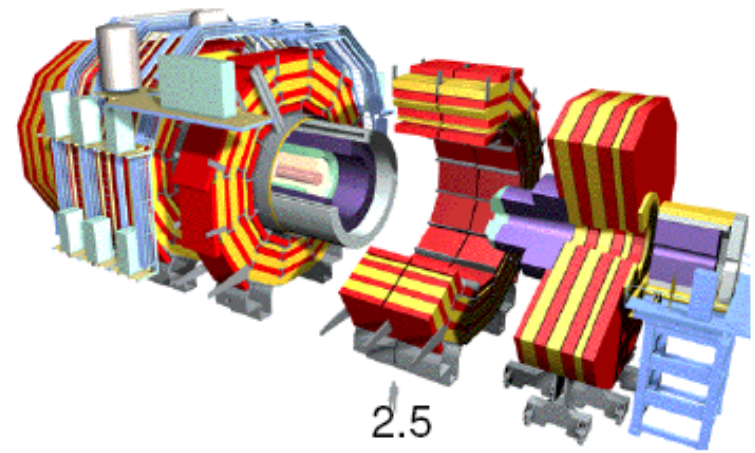

Inner tracker: $\lvert\eta\rvert$ coverage	2.5	2.5
$\sigma(p_T)/p_T$ at p_T=100 GeV	3.8%	1.5%
EM calorimeter: $\lvert\eta\rvert$ coverage	3.2	3.0
$\sigma(E)/E$	$9\%/\sqrt{E} + 0.5\%$	$3\%/\sqrt{E} + 0.25\%$
HAD calorimeter: $\lvert\eta\rvert$ coverage	4.9	5.2
$\sigma(E)/E$ (EM+HAD combined)	$70\%/\sqrt{E} + 3.3\%$	$70\%/\sqrt{E} + 8\%$
Muon system: $\lvert\eta\rvert$ coverage	2.7	2.4
$\sigma(p_T)/p_T$ at p_T=1 TeV	7%	5%

Physics at LHC

- Total cross section ~ 100-120 mb
- The goal at startup is to rediscover the *bread-and-butter* physics (i.e. QCD, SM candles)
  - σ_{jet} (p_T > 250 GeV)
    - 100 x higher than Tevatron
  - Electroweak
    - 10 x higher than Tevatron
  - Top
    - 10 x higher than Tevatron

- QCD processes not statistics limited!

- Startup Trigger menus are designed for L=8E29 and 1E31.

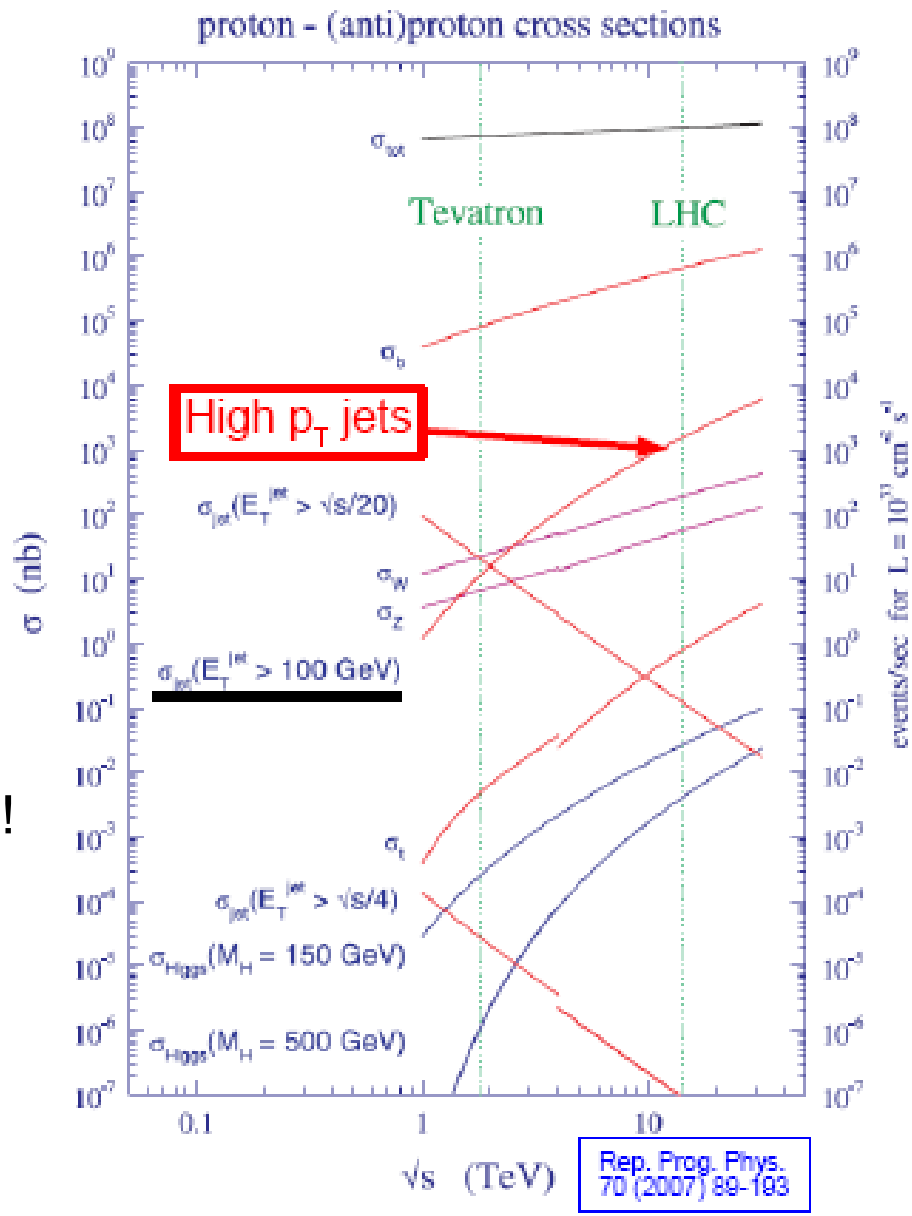

Tracker

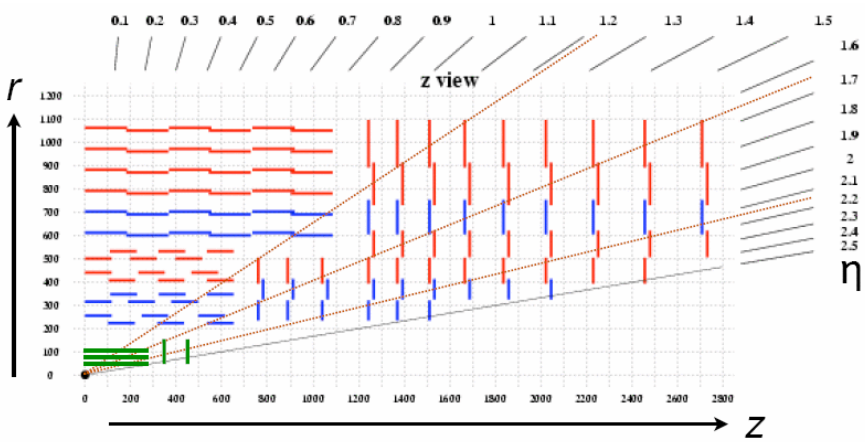

- Pixel layers, 3D measurements (green)
- Double sided strip modules, 3D measurements (blue)
- Single sided strip modules, 2D measurements (red)

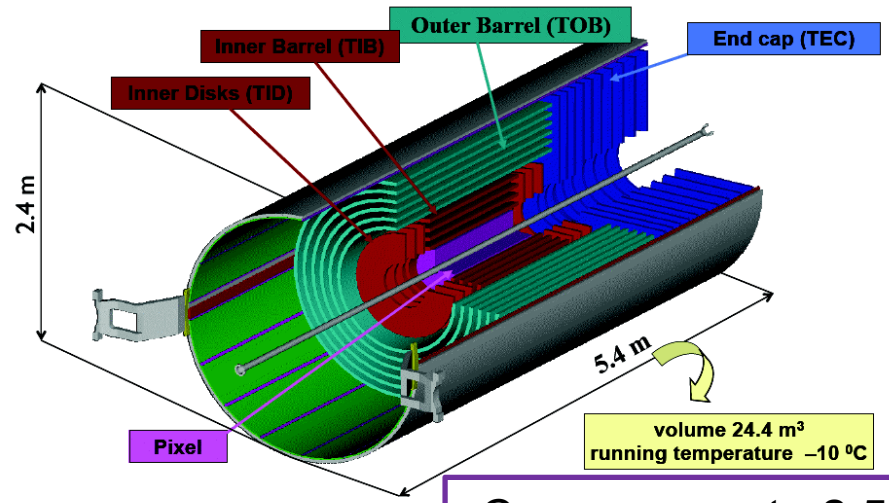

Coverage up to 2.5

- ❑ Pixel layers, 3D measurements (green)
- ❑ Double sided strip modules, 3D measurements (blue)
- ❑ Single sided strip modules, 2D measurements (red)

➢ Track reconstruction:

- Measure the true path of charged particle
- Measure the momentum (3-momentum)
- The sign of the charge of a particle
- With other constraints, the “origin” in space of the particle.

Preshower Detector

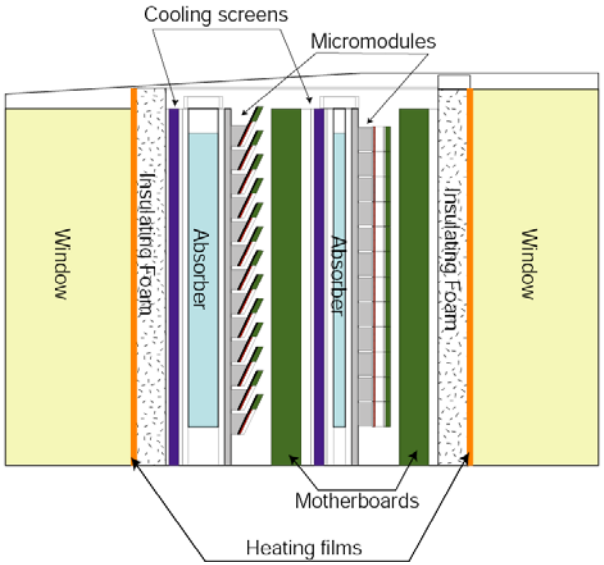

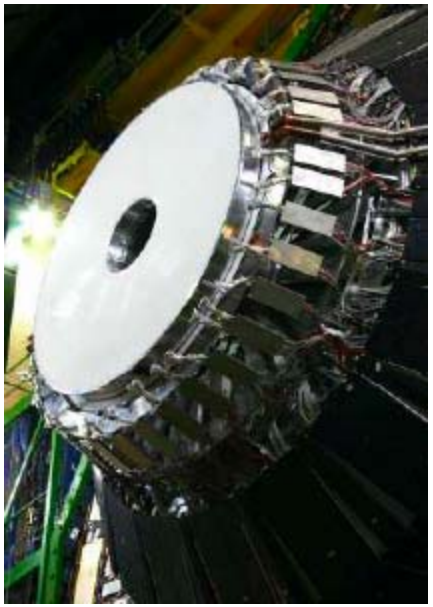

- Two layers of lead followed by silicon sensors placed in front of EE (1.6<η<2.6).
- 2mm Si strips to distinguish photons from π^0s and for vertex identification.

- Preshower Detector(ES) :
  - Two planes of lead absorber, measuring about 25cm x 25cm laterally. First plane (upstream in beam) approx 2X0 thick; second approx 1X0 thick.
  - Each ladder contains a 2 x 4 array of micromodules.
  - Thus there are 4 x 4 micromodules in each plane.
    - Total 32 Si-micromodules
  - Each micromodule is a combination of a 6.3cm x 6.3cm 320micron-thick silicon sensor divided into 32 strips mounted on ceramic and aluminium supports with attached front-end electronics.

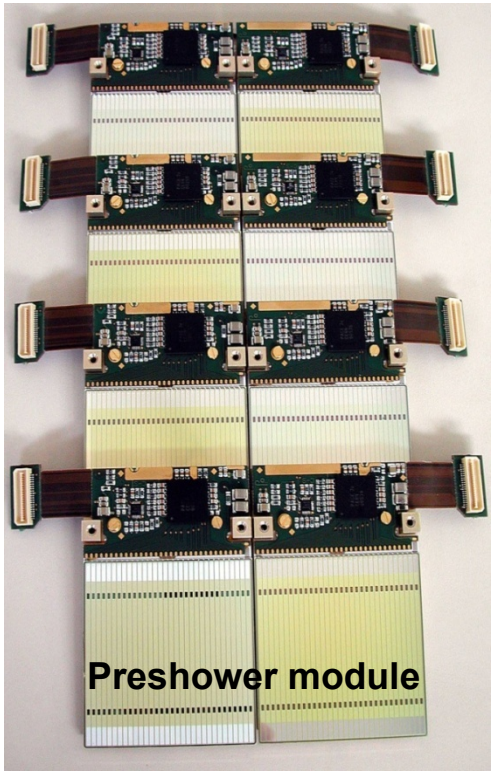

CK2/CK3 Pressure curves

Refractive Index : r(n) = c/n
CK2: 1.85 m long; CO_2 with 0.35 bar
No other particle gives signal in at this Pressure and efficiency > 99%

CK3: 1.85 m long; Freon at 0.88 bar
Used for beams < 3 GeV/c

Freon at 1.2 bar in order to separate Pion from Kaon and proton.

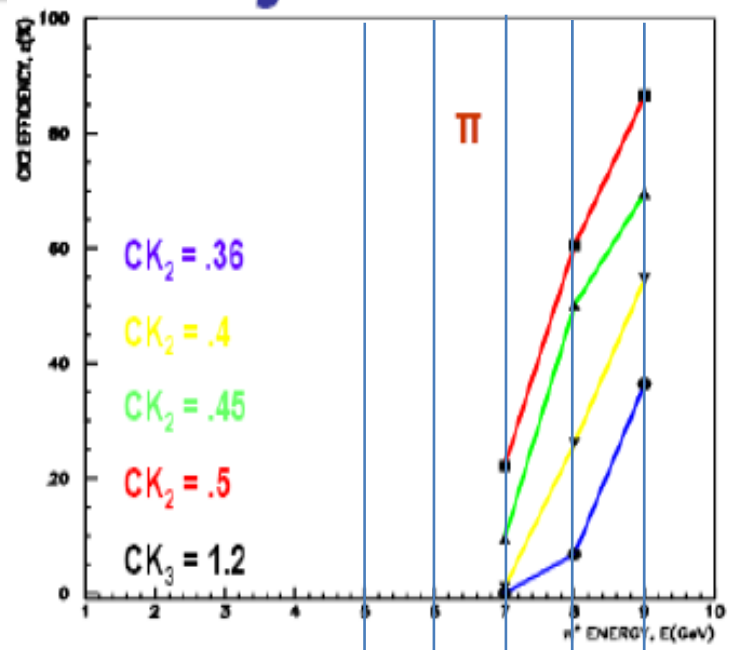

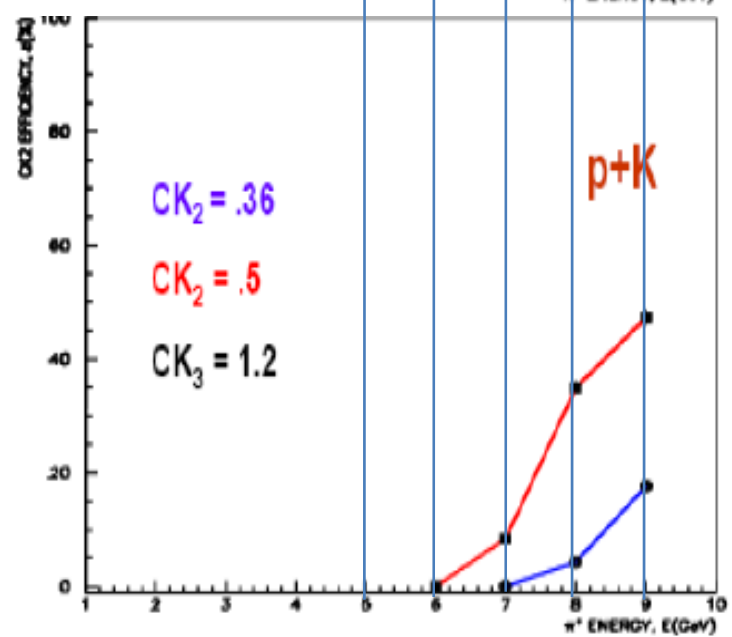

Calorimetry in particle physics

Energy resolution of the calorimeter:

a: stochastic term
b: noise term
c: constant term

$$\frac{\sigma_E}{E} = \frac{a}{E} \oplus \frac{b}{\sqrt{E}} \oplus c$$

a: Noise
Pile-up
b: Fluctuation in cascading
Photon statistics
c: Non Uniformity
Calibration uncertainty
Non confinement of shower

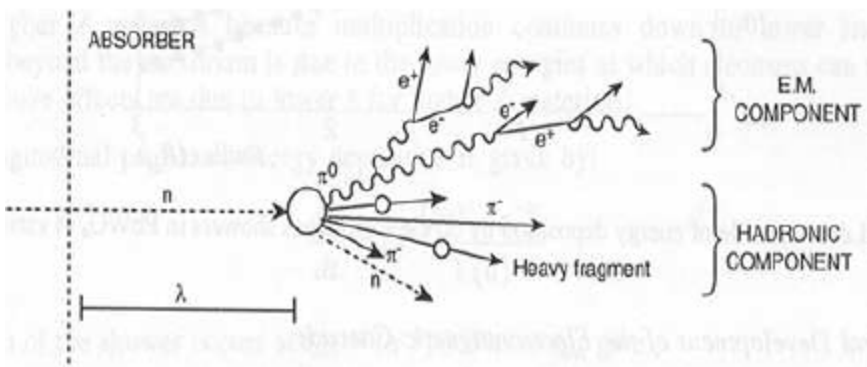

$$\frac{e}{\pi}(E) = \frac{e/h}{1 - \langle f_{em}(E) \rangle [1 - e/h]}$$

where e.m. fraction: $f_{em} \sim 0.1 \ln(E)$

What are different fluctuations in shower: (eg. Scintillation detector)

- thickness of scintillator
- uniformity of scinitillator properties
- position of shower center
- physics processes, charge particle / neutral particle
- energy sharing in active and passive material
- poisson fluctuation of produced photon
- absorption of photon in WLS fiber
- attenuation in fiber (surface quality, bending)
- loss in splicing junction
- quantum efficiency of HPD
- gain of HPD
- digitisation (analog to digital, loss of some information)
- fluctuation in timing measurement (TDC)
- fluctutation in pedestal level)

MET/$\sum E_T$

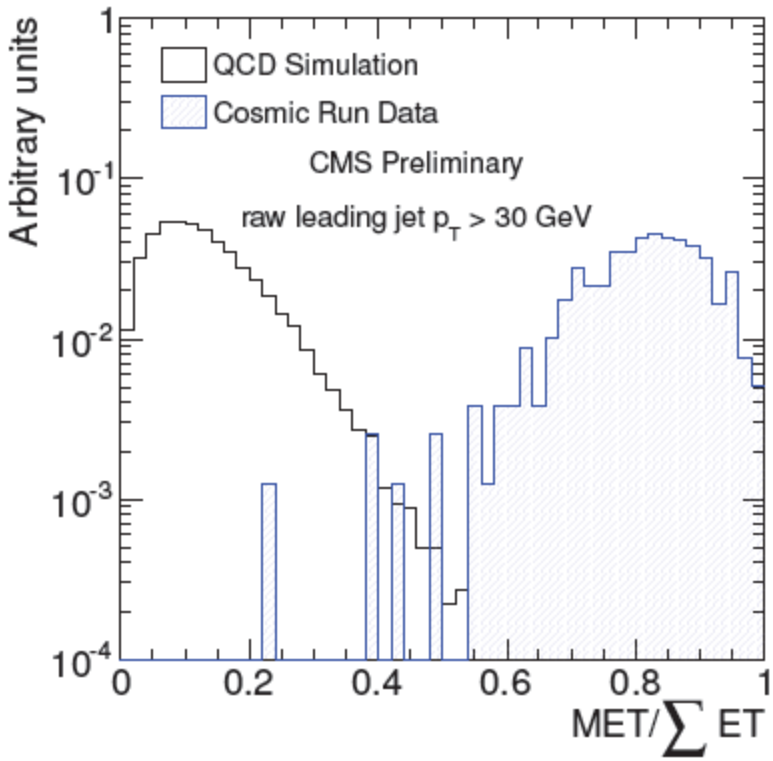

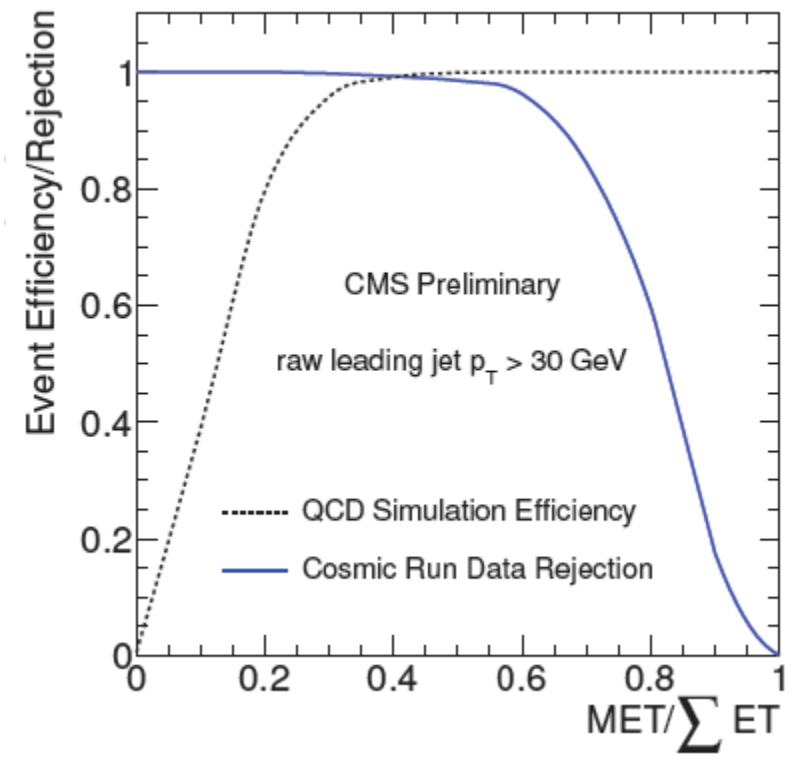

- <u>MET originates from:</u>

Large calorimeteric signals originating from noise
Beam halo energy deposits, Cosmic ray showers.

MET/$\sum E_T$ < 0.3
High rejection power +
Fully efficient (>99%) for events with sufficiently hard jets.

back

PYTHIA vs. HERWIG (modelling)

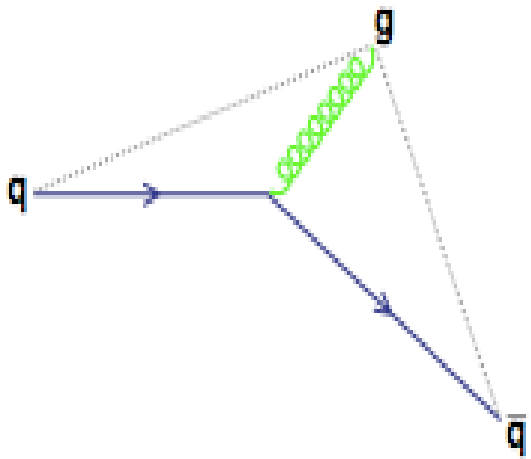

String representation of a $q\bar{q}g$ system. For such a system, where all the partons move apart from the common origin a string is stretched From the q end via the g to the $\bar{q}$ end.

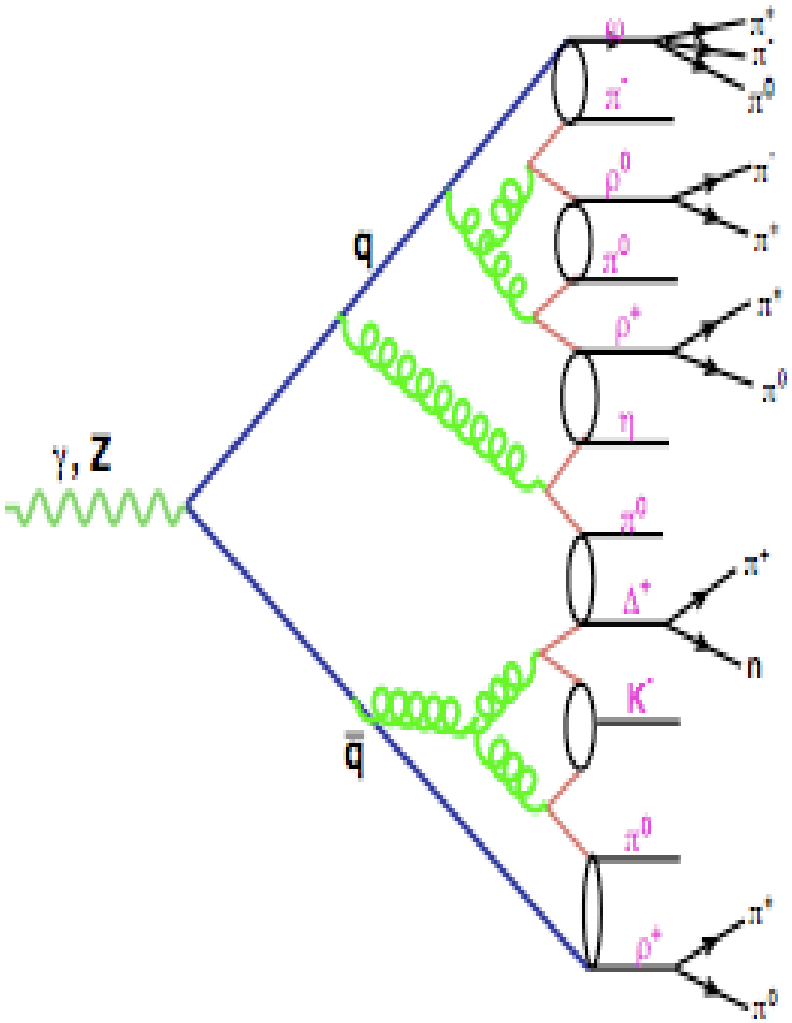

One cluster fragmentation scenario. Shower evolution is followed by forced $g \to q\bar{q}$ branching and formation of clusters which decay into hadrons.

Comparison of PYTHIA vs. HERWIG

PYTHIA: $Q^2 = m^2$	HERWIG: $Q^2 \sim E^2\theta^2$
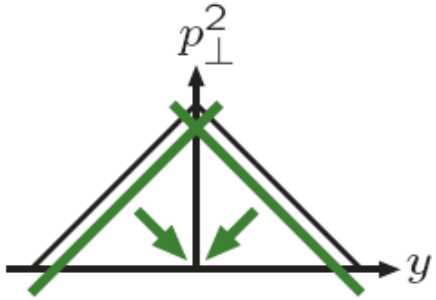	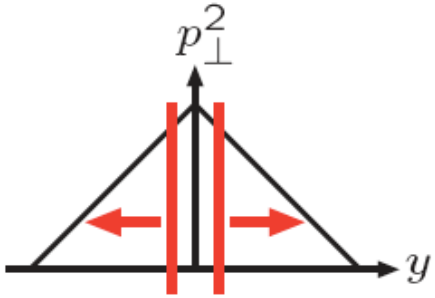
large mass first	large angle first
$\Rightarrow$ "hardness" ordered	$\Rightarrow$ **hardness not ordered**
coherence brute force	coherence inherent
covers phase space	**gaps in coverage**
ME merging simple	**ME merging messy**
$g \to q\bar{q}$ simple	$g \to q\bar{q}$ simple
not Lorentz invariant	**not Lorentz invariant**
no stop/restart	no stop/restart
ISR: $m^2 \to -m^2$	ISR: $\theta \to \theta$

Quark and Gluon jets

Quark & Gluon jets radiate proportionally to their color factor

- Jet profiles are sensitive to the quark/gluon jet mixture
  - Could separate quark and gluon jets in a statistical way

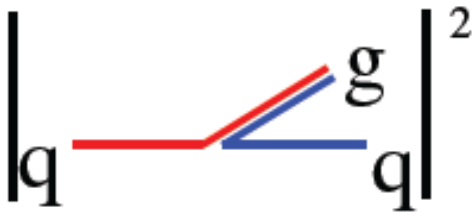

$\sim C_F = 4/3$

$\sim C_A = 3$

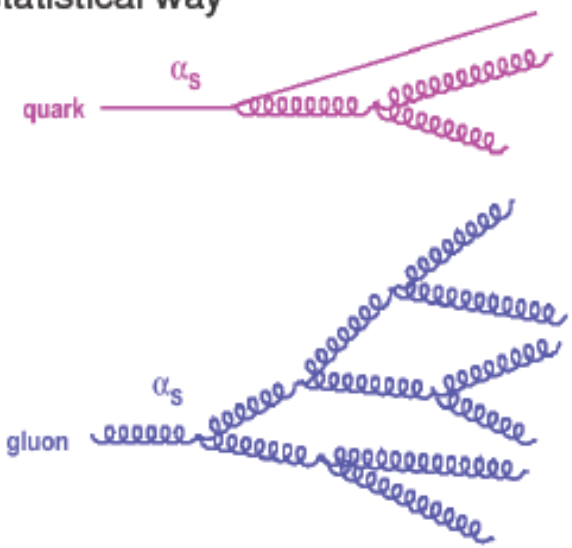

C_F ~ strength of a gluon coupling to a quark

C_A ~ strength of the gluon self coupling

At Leading Order ($E_{jet} \rightarrow \infty$):

$$r \sim \frac{C_A}{C_F} = \frac{9}{4} = 2.25$$

Color factors reflect basic properties of QCD.

Quark jets are narrower than the gluon jets due to the coupling strengths. Therefore the jets produced by quarks and gluons will show differences in their average multiplicity and the shape of the spectrum.

Why Matching? – Matrix elements vs. parton showers

Matrix elements	Parton showers
1. Fixed order calculation	1. Resums large logs
2. Computationally expensive	2. Computationally cheap
3. Limited number of particles	3. No limit on particle multiplicity
4. Valid when partons are hard and well separated	4. Valid when partons are collinear and/or soft
5. Quantum interference correct	5. Partial quantum interference through angular ordering
6. Needed for multi-jet description	6. Needed for hadronization/ detector simulation

Matrix element and Parton showers complementary approaches

Both necessary in high-precision studies of multijet processes

Need to combine them without double-counting!

Matching schemes

The simple idea behind matching

- Use matrix element description for well separated jets, and parton showers for collinear jets
- Phase-space cutoff to separate regions

This allows to combine different jet multiplicities from matrix elements without double counting with parton shower emissions

Difficulties

- Get smooth transition between regions
- No/small dependence from precise cutoff
- No/small dependence from largest multiplicity sample

- Matrix elements and parton showers - complementary descriptions of parton production:
  - ME needed to describe hard and widely separated jets
  - PS needed for very high multiplicities / substructure of jets / evolution to hadronization scale
- For realistic description of multijet backgrounds – necessary to combine descriptions: Matching!

MLM matching

M.L. Mangano [2002, Alpgen home page, hep-ph/0602031]

Use parton shower to choose events

1. Generate multiparton event with cut on jet $p_{T\min}$, $\eta_{\max}$ and $\Delta R_{\min}$, and factorization scale = "central scale" (e.g. transverse mass)
2. Cluster event (according to color) and use $d_i \simeq k_T^2$ for α_s scale
3. Shower event (using Pythia or Herwig) starting from fact. scale
4. Collect showered partons in cone jets with same $\Delta R_{\min}$ and $p_{T\mathrm{cut}} > p_{T\min}$
5. Keep event only if each jet matched to one parton
6. For highest multiplicity sample, allow extra jets with $p_T < p_{T\min}^{\mathrm{parton}}$

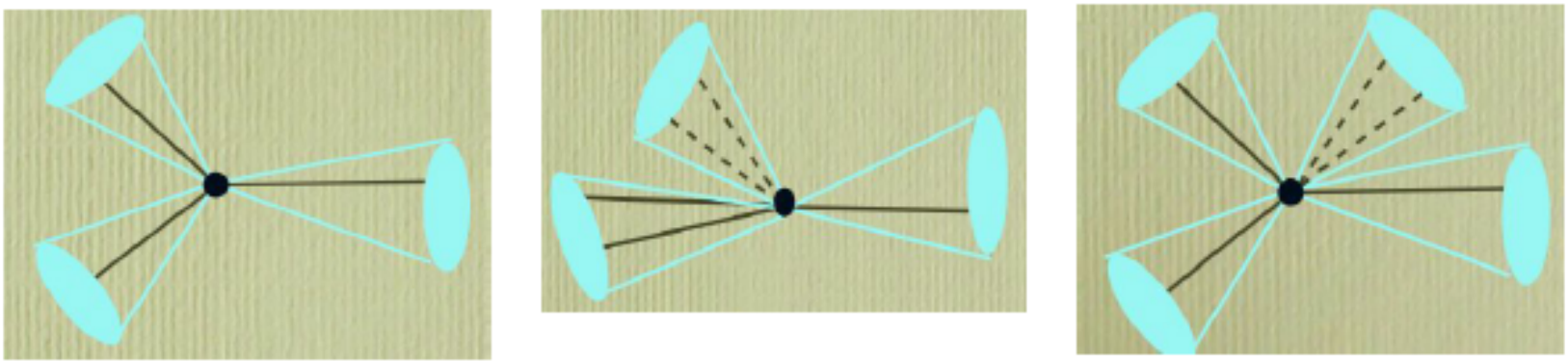

Keep | Discard | Keep only if highest multiplicity

Forward Detectors

- Add 2 calorimeters on either side covering larger |η| values, CASTOR (5.1 < |η| < 6.5) and the Zero Degree Calorimeter (ZDC). Both these have electromagnetic and hadronic section
- Complement with a tracking device (TOTEM) in the forward direction by adding telescopes and Roman Pot system

- CASTOR uses Quartz plates with tungsten absorbers of varying thickness – 2(10) em(had) sections with 2(4) mm quartz and 5(10) mm absorber.

- ZDC also uses tungsten with quartz fibres.and located at 140m from IP.

- TOTEM telescopes T1/T2 uses CSC/GEM and cover |η| = 3.2-5.0 & 5.0-6.6 respectively. Roman Pots are located at ±147m, ±180m and ±220m from IP each with 2 units 2.5m(4m) apart equipped with Si strip detectors

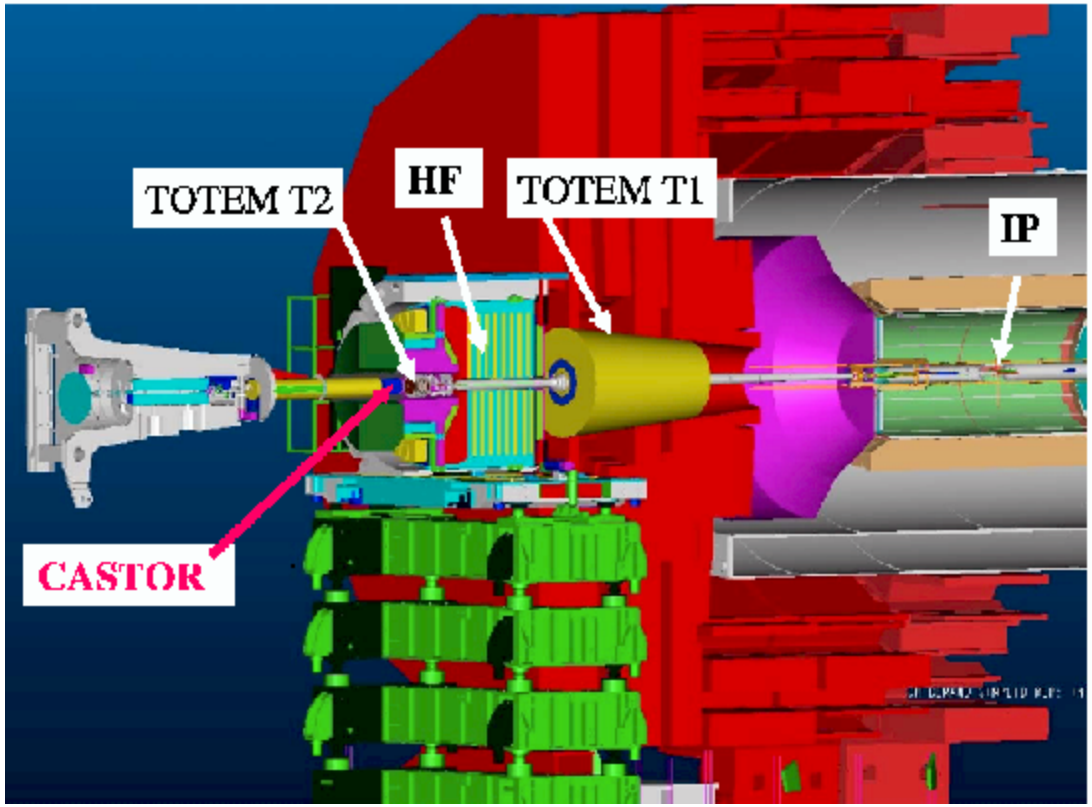

Jet Algorithms

A Jet algorithm is a set of mathematical rules that reconstruct unambiguously the properties of a jet.

❖ **Basic Jet Algorithm Requirements:**

1. Simple to use in experimental analyses and theoretical calculations.
2. Collinear safe.
The output of the jet algorithm remains the same if the energy of a particle is distributed among two collinear particles.
3. Infrared safe.
The output of the jet algorithm is stable against addition of soft particles.
4. Works in the presence of pile-up and underlying event contamination.

❖ **Jet Algorithm Types:**

1. Fixed Cone Algorithms
The jet is defined as a *cone* (with fixed radius in η-ϕ) in the direction of the dominant energy flow.
Eg. IterativeCone, SisCone.
2. Successive Recombination Algorithms ($\mathbf{k_T}$)
The construction of the jet is based on the angular coherence and transverse momenta of its constituents.

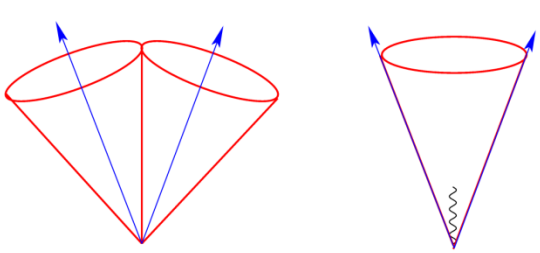

Infra red problem

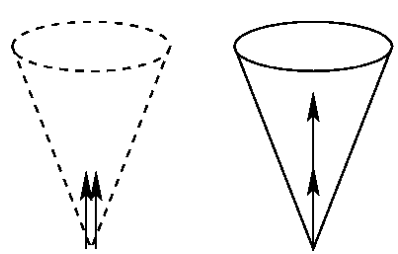

Collinear problem

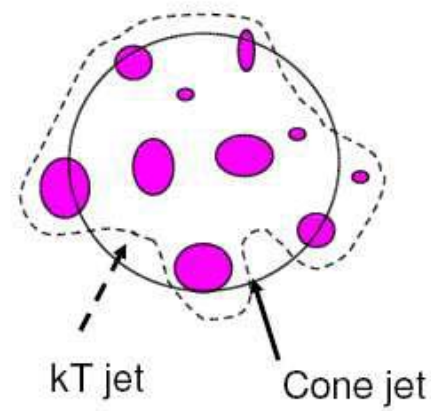

Event shape with 7 TeV CMS data

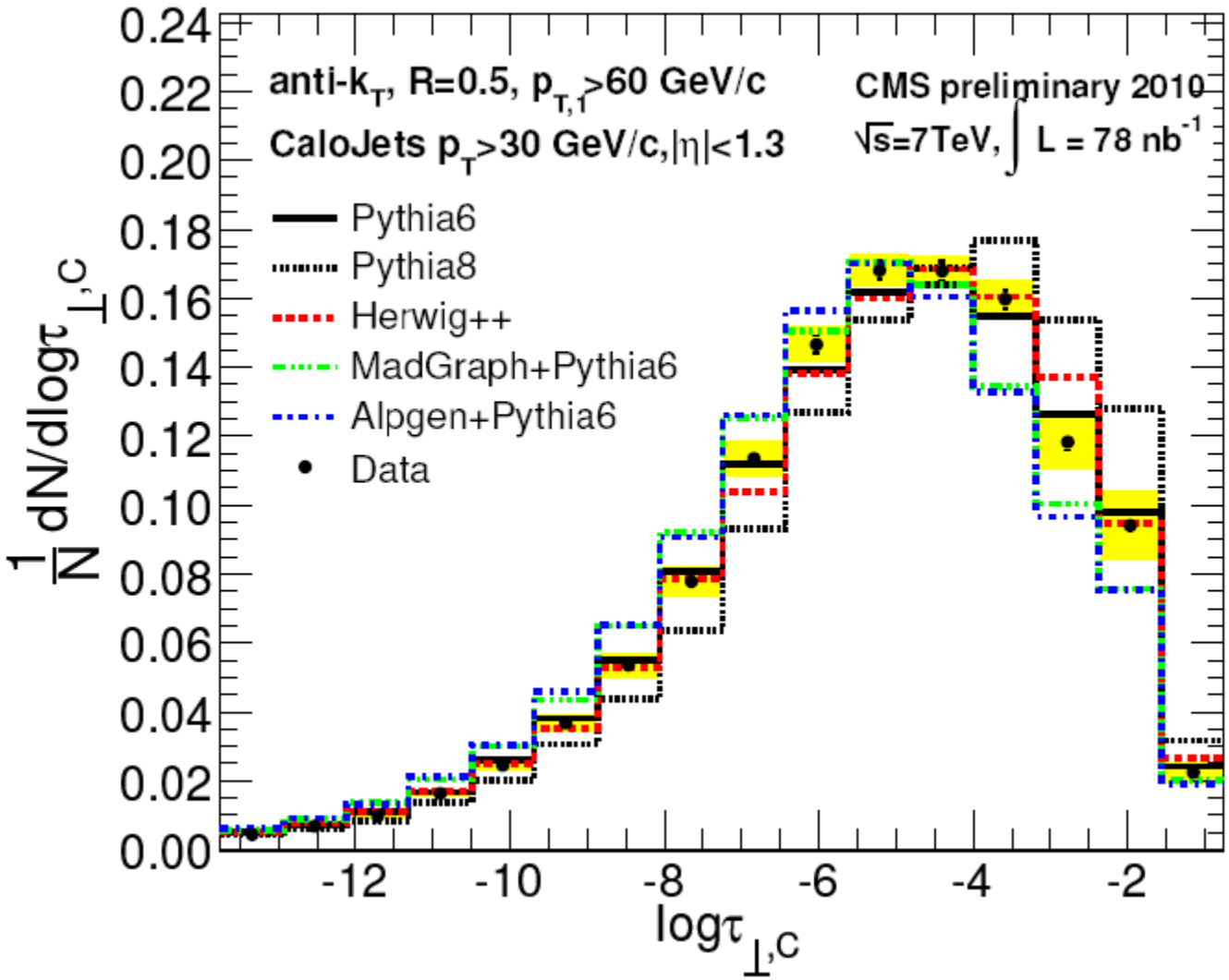

Ref: “Hadronic Event Shapes in pp Collisions at 7 TeV” (CMS PAS QCD-10-013)

QCD theory

The QCD Lagrangian

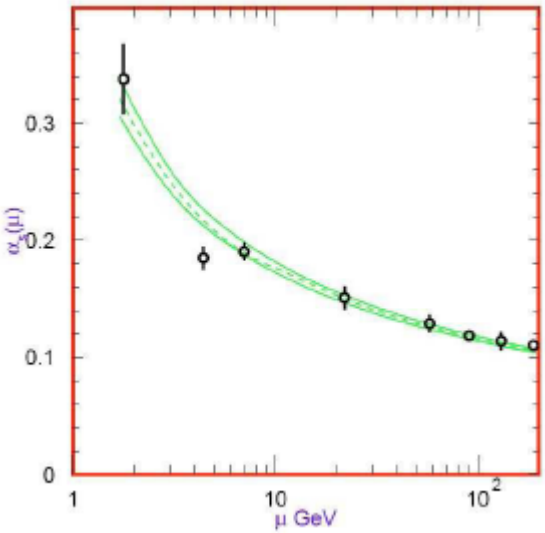

$$\mathscr{L} = -\frac{1}{4}(F^a_{\mu\nu})^2 + \bar{\psi}(i\not{D} - m)\psi + \mathscr{L}_{\rm GF}$$

where $a = 1, 8$ is an adjoint label.

Each flavour of quark transforms under the fundamental representation of $SU(3)$ and the gluons transform under the adjoint representation (as do all gauge bosons).

$$F^a_{\mu\nu} = \partial_\mu A^a_\nu - \partial_\nu A^a_\mu + g f^{abc} A^b_\mu A^c_\nu$$

f^{abc} are the structure constants of $SU(3)$

$$[T^a, T^b] = i f^{abc} T^c, \qquad D_\mu = \partial_\mu - i g A^a_\mu T^a$$

- Asymptotic Freedom $\Rightarrow$ we can make perturbative predictions in QCD for a large range of important hard processes.

$$\beta(g) \equiv \mu \frac{\partial g}{\partial \mu} = -\beta_0 \frac{g^3}{16\pi^2} - \beta_1 \frac{g^5}{(16\pi^2)^2} - \beta_2 \frac{g^7}{(16\pi^2)^3} - \cdots$$

- The key feature is that the first term is negative $\Rightarrow$ the coupling constant decreases with the scale "

$$\alpha_s(\mu) \equiv \frac{g^2(\mu)}{4\pi} = \frac{4\pi}{\beta_0 \log(\mu^2/\Lambda^2)} \left\{ 1 - \frac{\beta_1}{\beta_0^2} \frac{\log\left[\log(\mu^2/\Lambda^2)\right]}{\log(\mu^2/\Lambda^2)} + \frac{\beta_1^2}{\beta_0^4 \log^2(\mu^2/\Lambda^2)} \times \left(\left(\log[\log(\mu^2/\Lambda^2)] - \frac{1}{2} \right)^2 + \frac{\beta_2 \beta_0}{\beta_1^2} - \frac{5}{4} \right) \right\}.$$

Passage of particles through matter

relativistic charged particle passes though matter

$$-\frac{dE}{dX}\Big|_{ion} = N_A \frac{Z}{A} \frac{4\pi\alpha^2(\hbar c)^2}{m_e c^2} \frac{Z_i^2}{\beta^2} \left[\ln \frac{2m_e c^2 \gamma^2 \beta^2 T_{max}}{I^2} - \beta^2 - \frac{\delta(\beta\gamma)}{2} \right],$$

Electrons:

1. Ionization energy loss: low energy e^-/e^+. Bhabha, Moller etc.
2. Radiative energy loss: Brem. (radn in the columb field) : a few MeV.
   - directly proportional to Z^2. Hence more in heavier targets.
   - $\mathbf{E_c}$: E_ionisation = E_radiation.

Photons:

1. Photoelectric effect (<500 KeV).
2. Compton Scattering (100's KeV – a few MeV).
3. Pair-production (> $2m_e$ = 2x0.511 MeV).
4. Rayleigh scattering, photo-nuclear absorption.

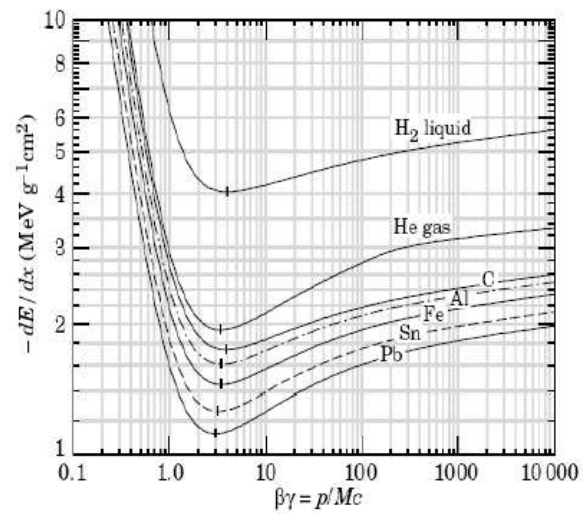

Hadrons:

1. EM component: π^0 and $\eta \rightarrow \gamma\gamma$
2. Nuclear spallation: incoming hadron makes quasi-free collisions with nucleons inside the nucleus.
3. Nuclear Binding Energy: cannot be converted to visible signal.
4. Neutron interaction: